Assessment of the branching quantification in poly(acrylic acid): Is it as easy as it seems?

Alison R Maniego, Adam T Sutton, Marianne Gaborieau, Patrice Castignolles

Assessment of the branching quantification in poly(acrylic acid): is it as easy as it seems?

Alison R. Maniego[1,2], Adam T. Sutton[1,2]†, Marianne Gaborieau[1,2],Patrice Castignolles[2]*

[1]Western Sydney University, Medical Sciences Research Group (MSRG), Parramatta, Australia

[2]Western Sydney University, Australian Centre for Research on Separation Sciences (ACROSS), School of Science and Health (SSH), Parramatta, Australia

AUTHOR INFORMATION

Corresponding Author

*E-mail: m.gaborieau@westernsydney.edu.au

Present Addresses

† AS Future Industries Institute (FII), University of South Australia, Mawson Lakes, South Australia 5011, Australia

KEYWORDS. Poly(acrylic acid), degree of branching, solubility, quantitative NMR spectroscopy, accuracy, precision

ABSTRACT

Branching in polymers is an important feature that plays a role in their applications. The degree of branching (*DB*) has been quantified in several polymers using NMR spectroscopy. In this work, the *DB* of poly(acrylic acid), PAA, was quantified. The precision and accuracy of *DB*

quantification in this polymer has been assessed for the first time. Incomplete dissolution lowers the accuracy of DB. Moisture content, chain end and impurities have to be taken into account to assess the solubility correctly. The incomplete solubility may be partially due to some clustering and it might for example explain the notable inaccuracy of the molecular weight determined by SEC for PAA. The error introduced during data treatment in NMR spectroscopy affects the precision of *DB*. This study enables the design of the best approach for a precise and accurate *DB* quantification not only for PAA but also for other branched polymers. An accurate *DB* increases the knowledge of the polymer structure enhancing the capacity to tailor PAA structures for properties desired in many applications.

TABLE OF CONTENTS GRAPHIC

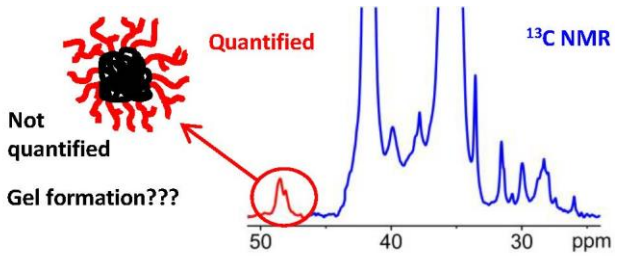

INTRODUCTION

Branching is a key structural feature of a number of important polymers such as starch, polyethylene or polyacrylics.[1] It plays a crucial role in the properties such as rheological properties[2] and interfacial properties.[3] Poly(acrylic acid), PAA, and its salt, poly(sodium acrylate), PNaA, are both branched polymers and important industrial polymers,[4] e.g. used in diapers[5] or water purification[6]. PAA and PNaA are also researched for drug delivery[7-15], and as an additive for the prevention of scaling.[16-19] Branching in PNaA is usually not introduced by design, but it was identified using ^{13}C NMR spectroscopy for PAA and PNaA obtained by

radical polymerization.[20-24] The likely presence of branching is still not taken into account for most publications about PAA. Intermolecular and intramolecular (chain) transfer to polymer result in a mid-chain radical which can lead to branching with a quaternary carbon (C_q) as the branching point. [20-22, 24]

NMR spectroscopy has been proven to be an effective tool for the degree of branching (*DB*) quantification of several branched polymers. *DB* quantification via the C_q signal has been carried out on polyolefins and polyacrylates using several ^{13}C NMR spectroscopy methods including solid-state[28, 30], swollen-state[30], melt-state[26, 30, 31] and solution-state[20, 21, 25, 27, 29, 30] NMR spectroscopy. For branching quantification in hydrophobic polyacrylates, solid-state NMR spectroscopy exhibited a too low resolution and swollen-state NMR spectroscopy a low sensitivity.[30] Melt-state NMR spectroscopy has shown high sensitivity and sufficient resolution for the *DB* quantification in polyolefins and hydrophobic polyacrylates.[26, 30, 31] Solution-state NMR spectroscopy also yields high-resolution spectra for hydrophobic polyacrylates, but with variable accuracy in the determination of *DB* assumingly due to the presence of microgels in some samples.[30]

Accuracy for the *DB* determination by quantitative NMR spectroscopy is challenging to assess due to the absence of calibration standards with known *DB*. For this reason, most *DB* measurements are self-calibrated with the area of the branching signal related to the area of the backbone signal in the same spectrum (without comparison with a known *DB* standard). The accuracy and precision of these self-calibrations were assessed for quantitative ^{13}C NMR measurements of ethylene/1-octene copolymers.[32] The reproducibility of these self-calibration schemes involved the comparison of quantitative ^{13}C NMR measurements of ethylene/1-octene copolymers determined using two different NMR spectroscopy instruments with similar experimental set-ups. Several simulations were also used to detect any error during data

treatment. The assessment of these self-calibration schemes is not restricted to ethylene/1-octene copolymers and should be applied to other branched polymers such as PAA.

DB quantification by NMR spectroscopy encountered several limitations impacting on the precision and accuracy, including systematic errors. The precision of the *DB* quantification depends on the number of scans (*NS*). Automated phase correction may also not be accurate with polymers due to their broad signals and possible baseline correction errors may lead to limitations in determining the *DB*.[33, 34] Manual processing can lead to errors as treatment routines may vary from user to user leading to slight differences in the applied phase and baseline correction in addition to the choice of the integration limits.[33, 34] The error caused by phasing in solid-state NMR spectroscopy was investigated for the degree of acetylation (*DA*) quantification in chitosan.[35] The relative standard deviation (*RSD*) from phasing was calculated by comparing several data sets phased by four different users. For the *DB* quantification in polyolefins, the reproducibility was improved by having a set protocol for the set-up and treatment of the data for all users.[33, 34]

The empirical method for the estimation of the *RSD* of *DB* established for polyolefins[33, 34] was applied to the *DB* of poly(*n*-alkyl acrylates)[30]. A theoretical approach for the calculation of the *RSD* of the *DB* was also proposed for poly(*n*-alkyl acrylates).[30] Limited differences were observed between the *RSD* values obtained using these empirical and theoretical approaches for the *DB* quantification in poly(*n*-alkyl acrylates), and the empirical method was found to overestimate the *RSD* of the *DB*s measured by solution-state NMR spectroscopy.

In this work, the *DB* of PAA/PNaAs synthesized with various reversible-deactivation radical polymerization (RDRP) methods as well as a Linear PAA and PAA obtained by radical polymerization was quantified using solution-state NMR spectroscopy. [29] PAAs/PNaAs obtained by several polymerization methods were chosen to have a wide range of samples for the

assessment of the precision and accuracy of the *DB* quantification in PAA/PNaA. Although it has been shown that melt-state NMR spectroscopy is the method of choice for *DB* quantification in polyolefins and hydrophobic polyacrylates[26, 30, 31], this method would demand very high temperatures to melt PAA. These temperatures, typically 150 °C above the glass transition temperature (T_g), are expected to degrade the PAA samples. Thermogravimetric analysis of PAA indeed indicated degradation above 200 °C[36] which is only 100 °C above PAA's T_g[37]. Thus, for this study solution-state NMR spectroscopy was selected as the only method currently available for PAA. It must however be noted that in solution-state NMR spectroscopy, gel fractions and/or clustered fractions that could be present in the sample may not be measured in the *DB* quantification as they are not solvated and mobile enough in solution. Therefore, possible errors introduced by incomplete sample dissolution and data processing were investigated in order to assess the precision and accuracy of *DB* quantification in PAA by solution-state NMR.

EXPERIMENTAL SECTION

Materials

Maleic acid (≥99 %), tetramethylsilane (TMS, 99 %), and trifluoroacetic acid (TFA, 99 %) were obtained from Sigma. Pyridine was supplied by Univar. 1,4-dioxane-d_8 (dioxane-d_8, 99 % D), deuterium oxide (D_2O, 99.9 % D), 40 % sodium deuteroxide (NaOD) in D_2O (99.5 % D), 35 % deuterium chloride (DCl) in D_2O (99.5 % D) and dimethyl sulfoxide-d_6 (DMSO-d_6, 99.9 % D) were sourced from Cambridge Isotope Laboratories, Inc.

Polymer synthesis

Samples codes are listed in Table 1. PAAs/PNaAs synthesized by nitroxide-mediated polymerization (NMP)[22], atom-transfer radical polymerization (ATRP)[17] and macromolecular design via interchange of xanthates (MADIX)[38] were obtained from Aix-Marseilles University

(France), University of New England (Australia), and Paul Sabatier University (France), respectively. Conventional PAA was also supplied by Aix-Marseilles University (France). The synthesis and SEC conditions were similar to published ones for samples synthesized with NMP[22], conventional radical polymerization [22], MADIX[38] and ATRP[16, 17]. A linear PNaA sample was purchased from Polymer Standard Service (Mainz, Germany, lot number paa26027). More information about the polymerization is given in the Supporting Information.

Thermogravimetric analysis (TGA)

TGA measurements were carried out on a STA 449C Jupiter (Netzsch). The samples were heated from room temperature to 120 °C at 10 °C·min^{-1} under a 25 mL·min^{-1} nitrogen atmosphere; an isotherm at 120 °C was then kept for 60 min. The moisture content was calculated from the weight loss at the end of the isotherm.[13]

Table 1. Description of poly(acrylic acid) samples investigated in this work. $M_{n,th}$ refers to the theoretical number-average molar mass, and $M_{n,SEC/NMR}$ to the number-average molar mass determined with SEC or NMR (as specified for each value). MONAMS refer to methyl 2-[*N*-tertiobutyl-*N*-(1-diethoxyphosphoryl-2,2-dimethylpropyl)aminoxy]propionate, BB to BlocBuilder, AIBN to 2,2'-azobisisobutyronitrile, ACBN to 1,1'-azobis(cyclohexanecarbonitrile), HB to hexyl 2-bromoisobutyrate, and HDB to hexadecyl-2-bromoisobutyrate

Sample	**Synthesis**	$M_{n,th}$ **(g·mol^{-1})**	$M_{n,SEC/NMR}$ **(g·mol^{-1})**	**Initiator**
NMP-AA-1	NMP	4,900	6,900 (SEC)[22]	MONAMS
NMP-AA-3	NMP	4,600	7,800 (SEC)	MONAMS
NMP-AA-5	NMP	2,100	10,000 (SEC)	BB
NMP-AA-6	NMP	2,700	12,000 (SEC)	BB
NMP-tBA-1	NMP of *t*-butyl acrylate and hydrolysis	13,100	7,500 (SEC)[22]	MONAMS
MADIX-AA-4	MADIX	10,000	22,000(SEC)	AIBN
MADIX-AA-5	MADIX	10,000	20,000(SEC)	ACBN
MADIX-AA-6	MADIX	10,000	17,000(SEC)	*t*-Butyl peroxide
ATRP-tBA-1	ATRP of *t*-butyl acrylate and hydrolysis	6,810	2,880 (SEC)[16] 4,220 (NMR)[16]	HB
ATRP-tBA-2	ATRP of *t*-butyl acrylate and hydrolysis	6,750	9,390 (NMR)[16]	HDB
CONV-AA-1	Conventional	n.d.[a]	33,700 (SEC)	AIBN
Linear	anionic polymerization of *t*-butyl acrylate and hydrolysis	n.d.[a]	39,300 (SEC)[22]	

[a]not determined

NMR spectroscopy

PAA and PNaA samples were dissolved for at least overnight at room temperature at different concentrations (69.9 – 200 $g \cdot L^{-1}$) in different solvents depending on the nature of the sample and heated if necessary when they looked cloudy (Table 2). Heated samples were heated at 60 °C whilst stirring at 300 rpm overnight in an Eppendorf Thermomixer C unless indicated otherwise. NMR spectra were recorded using a Bruker DRX300 spectrometer (Bruker Biospin Ltd, Sydney) equipped with a 5-mm dual $^{1}H/^{13}C$ probe, at Larmor frequencies of 300.13 MHz for ^{1}H and 75.48 MHz for ^{13}C, at room temperature (~ 25 °C). In 1,4-dioxane-d_8, the tetramethylsilane signal at 0 ppm was used as a reference for ^{1}H and ^{13}C chemical shifts. Samples dissolved in D_2O were externally calibrated to the methyl signal of ethanol in D_2O at 1.17 and 17.47 ppm for ^{1}H and ^{13}C chemical shifts, respectively.[39]

Table 2. Dissolution conditions and experimental parameters of ^{13}C NMR experiments.

Sample	Solvent	Concentration ($g \cdot L^{-1}$)	Heated	Number of scans (*NS*)	Repetition delay(s)	Dissolution test	DEPT-135 conducted (*NS*)
NMP-AA-1	Dioxane-d_8	150	No	45,056	6.00	No	Yes (15,360)
NMP-AA-3	Dioxane-d_8	150	No	37,328	7.00	Yes	No
NMP-AA-5	D_2O / NaOD[a]	149	No	45,948	6.00	Yes	No
NMP-AA-6	D_2O	100	No	45,948	6.00	Yes	No
NMP-AA-6	D_2O /NaOD	74.9	Yes	n.r.[c,d]	n.r.[c,d]	Yes	No
NMP-tBA-1	D_2O / NaOD [a] / DCl[b]	125	No	57,344	12.0[d]	Yes	Yes (36,272)
NMP-tBA-1	DMSO-d_6	69.9	No	27,653	6.00[d]	Yes	No
MADIX-AA-4	Dioxane-d_8	100	No	81,920	10.0	Yes	Yes (45,198)
MADIX-AA-5	Dioxane-d_8	200	Yes	16,774	10.0	Yes	Yes (22,770)
MADIX-AA-6	Dioxane-d_8	200	Yes	14,900	10.0	Yes	Yes (24,984)
ATRP-tBA-1	Dioxane-d_8	100	No	40,068	6.00	No	No
ATRP-tBA-2	Dioxane-d_8	100	No	13,107	6.00	Yes	No
CONV-AA-1	Dioxane-d_8	100	No	47,512	25.0	No	No
Linear	D_2O	100	No	n.r.[c,d]	n.r.[c,d]	No	No

[a]NaOD is 1 mol equivalent to acrylic acid (AA) units; [b]DCl is ½ mol equivalent to AA units; [c]spectrum was not recorded; [d]*DB* was not quantified

Quantitative one dimensional (1D) ^{1}H NMR spectra were recorded with a 10,000 Hz spectral width, a 30° flip angle, 50 s repetition delay and 40 scans. ^{13}C NMR spectra were recorded with a 20,000 Hz spectral width, inverse-gated decoupling, a 90° flip angle, repetition delays of 6 to 7 s and 13,107 to 81,920 scans (Table 2). Repetition delays were set at least five times longer than the longitudinal relaxation ($5T_1$) for the signals of interest (quaternary signal, C_q, the backbone signals, the signals overlapping the backbone and the signal corresponding to the carboxylic acid signal of the polymer) in order to ensure that the spectra obtained were quantitative (for more information on relaxation time estimation see supporting information, Figure S1). For the dissolution tests, $5T_1$ were set all the signals. ^{13}C distortionless enhancement by polarization transfer 135 (DEPT-135) spectra were recorded with a 20,000 Hz spectral width, a variable 135 ° ^{1}H flip angle, and the same repetition delay as for the quantitative ^{13}C NMR spectrum of the same sample. Maleic acid (100.00 g·L^{-1}) and pyridine (100.00 g·L^{-1}) in 1,4-dioxane-d_8 and D_2O, respectively, were used as internal standards to quantify the dissolution of several PAAs/PNaAs. The internal standard solutions were placed in a separate internal tube (internal diameter = 1.3 mm; outer diameter = 2.0 mm) to avoid interaction with the polymer in the main NMR tube (internal diameter = 4.2 mm).

RESULTS AND DISCUSSION

DB of several PAAs/PNaAs was quantified using ^{13}C NMR spectroscopy. The influence of dissolution and systematic errors in NMR measurements were investigated in order to improve the precision and accuracy of the *DB* quantification in PAAs and PNaAs. In order to confirm the presence of branching and the chemical structure of the PAAs/PNaAs in this study, structure elucidation of the polymers was conducted first.

^{13}C NMR signal assignment

1D ^{13}C NMR spectra were recorded for most PAA and PNaA samples. The CH_2, CH, and carboxylic acid groups of the linear sections of the polymer chains were found to have chemical shifts of 32.1 – 43.0, 39.1 – 49.4 and 167.8 – 190.3 ppm, respectively (Figure 1 and Figure S2 to S10). The detailed signal assignment of ^{13}C NMR spectra of NMP, MADIX, ATRP and conventional PAAs and PNaAs is shown in the supporting information (Figure S2 to S10 and Table S1 –S6). The signal between 46.1 and 50.9 ppm was assigned to the C_q which indicates the presence of branching in all PAAs/PNaAs (except the Linear). This signal was further confirmed using ^{13}C DEPT-135 NMR spectroscopy (Figure 1c). DEPT experiments were performed on most PAA/PNaA samples in order to confirm some signals with carbon-containing functional groups.

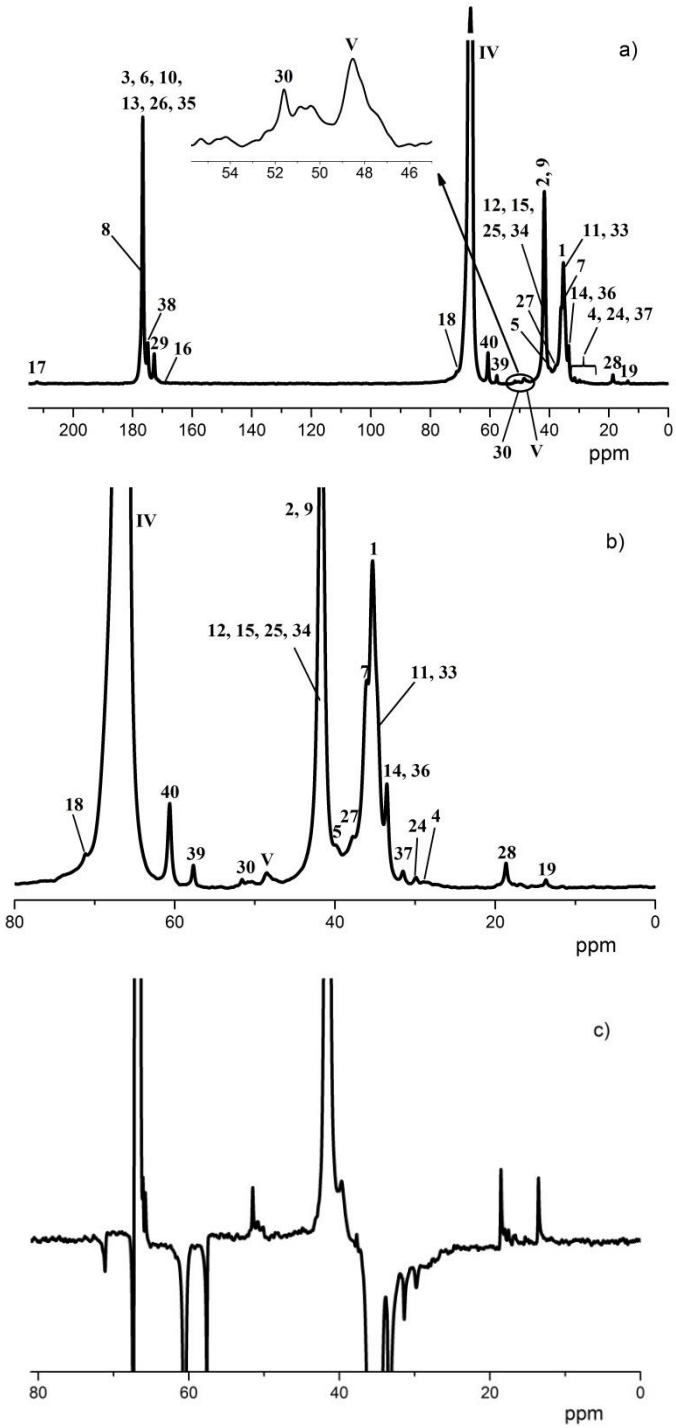

Figure 1. Solution-state ^{13}C NMR spectra (75.48 MHz) of MADIX-AA-4 in dioxane-d_8: a) full quantitative spectrum with insert showing the region of the C_q signal of the branching point (signal V), b) 0 to 80 ppm region of quantitative ^{13}C NMR spectrum and c) 0 to 80 ppm region of

DEPT-135 spectrum. See Figure S12, S13a, S14b and S14c for the chemical structure and Table S3 for the signal assignment.

Determination of the average degree of branching (*DB*) in PAA/PNaA via ^{13}C NMR spectroscopy

DB is the percentage of monomer units that are branched. It can be calculated using Equation 1[30]:

$$DB(\%) = \frac{I(\mathrm{C_q}) \cdot 100}{I(\mathrm{C_q}) + \frac{I(\mathrm{CH+CH_2})}{2}} \quad (1)$$

where $I(\mathrm{C_q})$ is the integral of the $\mathrm{C_q}$ signal at the branching point and $I(\mathrm{CH+CH_2})$ is the integral of the signals of the CH and $\mathrm{CH_2}$ backbone present in all monomer units. The NMR conditions for the *DB* quantification in PAAs and PNaAs are described in Table 2. An alternative calculation of the *DB* was used as shown in Equation 2:

$$DB(\%) = \frac{I(\mathrm{C_q}) \cdot 100}{I(\mathrm{C{=}O})} \quad (2)$$

where $I(\mathrm{C{=}O})$ is the integral of the signals of all carbonyl groups present in the main chain of the polymer (excluding end groups). Both approaches were taken during the *DB* quantification and their results compared for the validation of the values obtained. Equation 1 and 2 were modified for spectra that show signals overlapping with the ones present in Equation 1, in particular signals from the end group (Equation S3 - S18). All measurements were quantitative since the repetition delay was set to allow full relaxation between scans for all signals of interest (Figure S1).

Assessment of the precision of *DB* due to limited signal-to-noise ratio

The limited precision of the determined *DB* values due to the limited *SNR* is the signal-to-noise ratio of the C_q signal can be expressed through their relative standard deviation RSD_{SNR}[30]:

$$RSD_{SNR}(\%) = \frac{238}{SNR^{1.28}} \quad (3)$$

Equation 3 requires a *SNR* value which can be measured on a recorded spectrum or estimated for a published spectrum. Its applicability for the assessment of the precision of *DB* quantification for other polymers than the polyolefins it was empirically developed for has been discussed by Castignolles *et al*.[30]. At higher *SNR* values, other factors than the limited sensitivity of the C_q signal are expected to play a more and more significant role. Thus, *RSD* from data treatment, in particular phasing (RSD_{phas}) has also been investigated and will be discussed in more detail below.

Assessment of the precision of *DB* due to data treatment

DB of PAA has been quantified. [20, 21, 24, 40] However, the importance in assessing the error introduced during data treatment was overlooked. The *RSD* value calculated from the *SNR* (Equation 3) does not take into account the errors introduced by phasing which is especially important when the *SNR* is poor. In this work, 4 different users phased a set of 5 ^{13}C spectra (NMP-AA-1, NMP-AA-5, MADIX-AA-6, ATRP-tBA-1 and Conv-AA-1). *DB* was then quantified from these spectra to calculate the *RSD* from phasing, RSD_{phas}. *RSD* from phasing and *RSD* from *SNR* were compared (Figure 2). This relationship between the RSD_{phas} and RSD_{SNR} was also investigated for the *DA* quantification of chitosan samples.[35]

Since both *RSD*s are significant, it is important to take both into account. Assuming the correlation between both *RSD*s is linear (Figure 2), the following empirical equation was used in this work to assess the total *RSD* of the determined *DB* values:

$$RSD_{\mathrm{tot}}(\%) = RSD_{\mathrm{SNR}} + RSD_{\mathrm{phas}} = RSD_{\mathrm{SNR}} + 0.301 \cdot RSD_{\mathrm{SNR}} + 5.23 \quad (4)$$

$$RSD_{\mathrm{tot}}(\%) = \frac{310}{SNR^{1.28}} + 5.23 \quad (5)$$

Unlike the correlation of errors in the *DA* quantification[35], the coefficient of determination for the RSD_{phas} and RSD_{SNR}, r^2 was poor (0.465 vs 0.79). It must be noted that the *DA* quantification in chitosan was done with solid-state NMR spectroscopy whilst the *DB* quantification of PAAs/PNaAs were with solution-state NMR spectroscopy. In solid-state NMR spectroscopy, the resolution of the spectra and the chemical shifts of the different chitosan samples are very similar due to the absence of solvent which can cause a shift in signals.[35] This might explain the better linear correlation of RSD_{phas} with RSD_{SNR} in the case of the *DA* quantification.

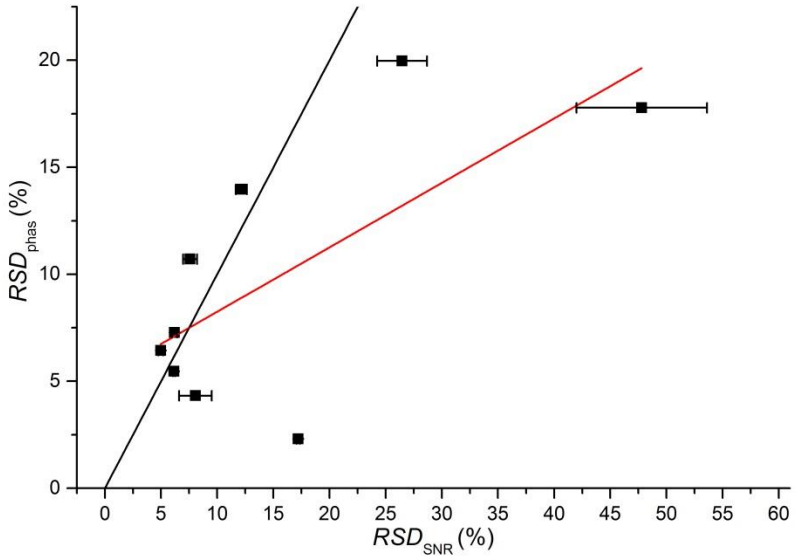

Figure 2. Comparison of errors originating in the limited *SNR* and in the data treatment (phasing) for the DB quantification of PAAs/PNaAs. The linear fit is shown in red (y = 0.301x + 5.23, R^2 = 0.465), and the diagonal in black.

Accuracy of *DB*: How to assess PAA/PNaA dissolution

A complete dissolution is achieved when the polymer chains are completely surrounded by molecules of solvent. An incomplete dissolution of a sample would result in having only a portion of the sample assessed for any solution-state NMR measurement, thus lowering the accuracy of the *DB* quantification. The average *DB* values obtained by solution- and melt-state ^{13}C NMR in the case of polyacrylates were not significantly different.[30] The incomplete dissolution of hydrophobic polyacrylates did not seem to be biased with respect to branching for samples that were relatively well soluble (obtained by solution polymerization), but it prevented the *DB* quantification with solution-state NMR in samples that were poorly soluble (obtained by emulsion polymerization). Dissolution of starch[41] and chitosan[35] was assessed using ^{1}H NMR spectroscopy. Obtaining a clear solution does not prove that the sample is fully dissolved.[41] Thus, a quantitative assessment is essential in order to portray a reliable verdict on a sample's solubility. The dissolution of PAA and PNaA and its influence on the accuracy of the *DB* quantification had not been investigated to our knowledge. It was assessed based on the principle that (^{1}H) solution-state NMR only detects dissolved species.[41] The amount of sample dissolved can be determined in two ways: through the peak area-to-noise ratio (*PNR*) of the sample signal or through the percentage of sample which dissolved determined by comparison with an internal standard.

The *PNR* could be used to compare samples in terms of their extent of dissolution, after it is normalized with respect to the number of scans and the nominal sample concentration (Equation S19). It has the advantage of not requiring an internal standard. The extent of solubility in PAAs obtained by conventional radical polymerization were assessed by quantifying the *PNR*.[24] The *PNR* was similar between linear and PAA without chain transfer agent (CTA) suggesting an almost complete dissolution with the assumption that Linear PNaA was completely soluble.

However poor *PNR* was observed for PAAs with CTA in comparison to those of Linear suggesting a poor solubility for these samples. The lower solubility for these samples may be due to the presence of sulphur in the thioester end group for PAAs with CTA. To assess the precision of the *PNR* method for this work, the normalized *PNR* values were compared for several samples in which toluene was present at the same concentration[41] (Figure S15). Large variations between the normalized *PNR* values were observed (in different starch suspensions: maize starch: *RSD* (%) = 24 %, n = 8; maize starch + LiBr: *RSD* (%) = 24 %, n = 6; Hom rice flour: *RSD* (%) = 11 %, n = 6; Makfay rice flour: *RSD* (%) = 7.5 %, n = 3). Therefore this method does not provide a precise estimate of the extent of a sample's dissolution. It was thus decided to use an internal standard to assess the extent of dissolution of several PAAs/PNaAs.

Several criteria must be taken into account in choosing a good internal standard. The internal standard must be pure, non-volatile, fully soluble in the solvent of the ^{1}H NMR measurement, and stable in the experimental conditions set during measurements in order to achieve a high precision of the quantity dissolved.[41] Furthermore, there should be at least one region of the ^{1}H NMR spectrum in which the internal standard signal does not overlap with any of the signals of interest of the polymer, and vice versa, in order to quantify both signals independently.[41] Internal standards used in this work that fulfill the criteria mentioned above were maleic acid and pyridine. Their solutions were placed in a separate internal tube in order to avoid interaction with the polymer.

The extent of dissolution of the sample as a percentage ($\%_{\mathrm{diss}}$) was quantified as the ratio of the molar concentration of the sample quantity dissolved (C_{diss}) to the sample molar concentration introduced initially:

$$\%_{\mathrm{diss}} = \frac{100 \times C_{\mathrm{diss}}}{C_{\mathrm{nom}}(1-mc)(1-f_{\mathrm{eg}})(1-f_{\mathrm{AA}})} \quad (6)$$

where C_{nom} is the nominal concentration of sample prepared (in g·L^{-1}), *mc* is the sample's moisture content (expressed as a mass fraction),f_{eg} is the mass fraction of end groups in the weighed PAA/PNaA sample and f_{AA} is the mass fractions of the acrylic acid (AA)..

C_{diss} can be determined as:

$$C_{\mathrm{diss}} = \frac{C_{\mathrm{St}} \cdot M_{PAA} \cdot I(\mathrm{PAA}) \cdot H_{\mathrm{St}} \cdot V_{\mathrm{St}}}{M_{St} \cdot I(\mathrm{St}) \cdot H_{\mathrm{PAA}} \cdot V_{\mathrm{PAA}}} \quad (7)$$

where C_{St} is the mass concentration of the internal standard, I(PAA) is the integral of the backbone signal of PAA/PNaA and I(St) are is the integral of the signal of interest of the internal standard. H_{PAA} and H_{St} are the number of protons corresponding to the signal of interest of PAA/PNaA and that of the internal standard, respectively, V_{PAA} and V_{St} are the volumes of PAA/PNaA and of internal standard solutions measured, respectively. Since the internal standard is in a smaller NMR tube within the NMR tube containing the PAA/PNaA solution the volumes are not the same. M_{PAA} and M_{St} are the molar mass of the acrylic acid/sodium acrylate monomer unit and of the internal standard, respectively.

The ratio of the measured volumes of the PAA/PNaA and standard solutions is equal to the ratio of their area (both having the same length):

$$\frac{V_{\mathrm{St}}}{V_{\mathrm{PAA}}} = \frac{\pi(id_{\mathrm{St}}/2)^2}{\pi(id_{\mathrm{PAA}}/2)^2 - \pi(od_{\mathrm{St}}/2)^2} \quad (8)$$

where id_{PAA} is the internal diameter of the NMR tube containing the PAA/PNaA solution, and id_{St} and od_{St} are the internal and outer diameters of the internal tube containing the internal standard solution, respectively. Combining Equations 6 to 8 yields:

$$\%_{\mathrm{diss}} = \frac{100 \times C_{\mathrm{St}} \cdot M_{AA} \cdot I(\mathrm{PAA}) \cdot H_{\mathrm{St}} \cdot \pi(id_{\mathrm{St}}/2)^2}{C_{\mathrm{nom}}(1-mc)(1-f_{\mathrm{eg}})(1-f_{\mathrm{AA}}) \cdot M_{St} \cdot I(\mathrm{St}) \cdot H_{\mathrm{PAA}} \cdot [\pi(id_{\mathrm{PAA}}/2)^2 - \pi(od_{\mathrm{St}}/2)^2]} \quad (9)$$

the moisture content *mc* measured by TGA (Figure S21), and the mass fraction of end groups f_{eg} are listed for all PAAs/PNaAs in Table S8. The molar masses are 72.06 g·mol^{-1} for acrylic

acid and 94.05 g·mol^{-1} for sodium acrylate (M_{AA}), and 116.1 g·mol^{-1} and 79.10 g·mol^{-1} for the internal standards (M_{St}, maleic acid and pyridine respectively). Representative ^{1}H NMR spectra are shown on Figure S19 to S21. For dissolution quantification, the signals of the PAA/PNaA backbone (≈ 0.29 – 3.0 ppm, H_{PAA}= 3), and of vinylic hydrogens of the maleic acid (≈ 6.3 ppm, H_{St}= 2) or of γ-CH of the pyridine (≈ 7.8 ppm, H_{St} =1) were used. The internal standard concentrations and the NMR tube diameters are given in the experimental section.

A AA dimer can form via Michael addition reaction, 2-carboxyethyl acrylate (CA).[42] A signal corresponding to the 2-carboxyethyl moiety is detected for NMP-AA-3 and MADIX-AA-6. However, no o free dimer was detected as minimal to no independent vinylic signals were detected (e.g. Figure S-7). The dimer may have copolymerized with AA. When a copolymer of the AA dimer and acrylic acid is observed, the expression of $\%_{diss}$ is modified through the replacement of M_{AA} with M_{PAA}:

$$\%_{\mathrm{diss}} = \frac{100 \times C_{\mathrm{St}} \cdot M_{PAA} \cdot I(\mathrm{PAA}) \cdot H_{\mathrm{St}} \cdot \pi(id_{\mathrm{St}}/2)^2}{C_{\mathrm{nom}}(1-mc)(1-f_{\mathrm{eg}})(1-f_{\mathrm{AA}}) \cdot M_{St} \cdot I(\mathrm{St}) \cdot H_{\mathrm{PAA}} \cdot [\pi(id_{\mathrm{PAA}}/2)^2 - \pi(od_{\mathrm{St}}/2)^2]} \quad (10)$$

with M_{PAA} defined as:

$$M_{PAA} = M_{AA} \cdot f_{AA\,unit} + M_{CA} \cdot f_{CA\,unit} \quad (11)$$

where $f_{AA\ unit}$ and $f_{CA\ unit}$ are the molar fractions of the AA and CA units respectively, and M_{CA} is the molar mass of the CA unit (144.12 g·mol^{-1} and 166.11 g·mol^{-1} for CA and sodium CA units, respectively). $f_{CA\ unit}$ can be defined using the integral of the independent signal of the CA unit (I(CA), H_{CA} = 2):

$$f_{\mathrm{CA\ unit}} = \frac{I(\mathrm{CA})/H_{\mathrm{CA}}}{[I(\mathrm{PAA}) - I(\mathrm{CA})]/H_{\mathrm{PAA}}} \quad (12)$$

Accuracy of *DB*: Assessment of the PAAs/PNaAs dissolution

The dissolution of PAAs/PNaAs was assessed using ^{1}H solution-state NMR spectroscopy (see Figure S16 to S18 for typical ^{1}H NMR spectra). Conditions for the sample dissolution prior to ^{1}H NMR spectroscopy are indicated in Table S8. The extent of dissolution ($\%_{diss}$) was determined for several PAAs and PNaAs (Figure 3a). To estimate the error on $\%_{diss}$, several ^{1}H NMR data sets were phased by 4 different users to determine the RSD_{phas}. No correlation was observed between RSD_{SNR} and RSD_{phas} (Figure S19). The error was mostly introduced by RSD_{phas} while RSD_{SNR} was negligible. Thus, the error bars for the determined $\%_{diss}$ are based on the highest RSD_{phas} which was 17.0 %.

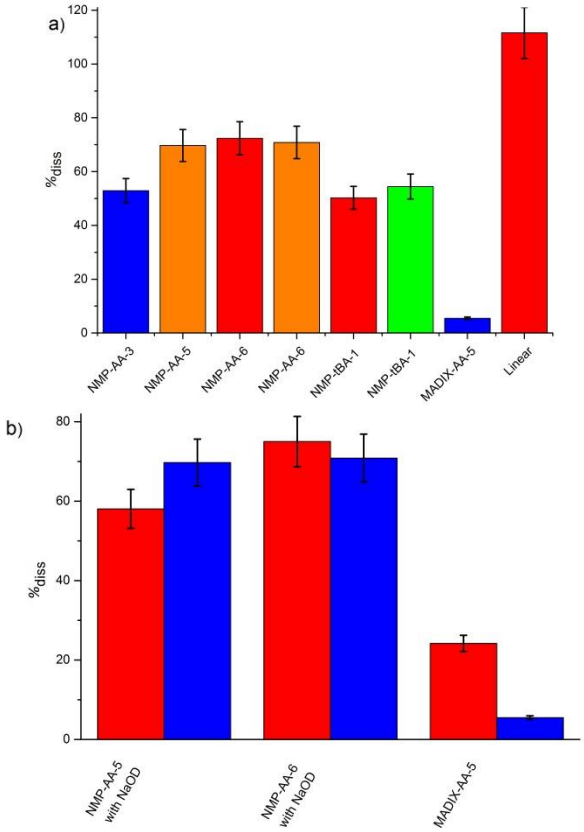

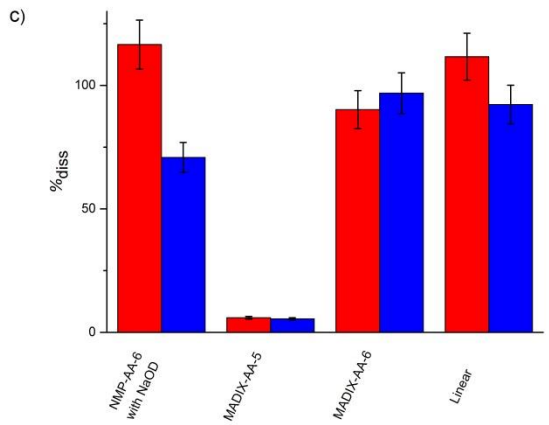

Figure 3. Extent of dissolution of PAAs and PNaAs: a) comparison of different samples in different solvents, dioxane-d_8 (blue), D_2O with NaOD (orange), D_2O (red) and DMSO-d_6 (green), using maleic acid as an internal standard (with the exception of linear PNaA which uses pyridine as an internal standard); b) comparison between the initial concentration given in Table S7 (blue) and a ten-fold lower concentration (red) using maleic acid as an internal standard; c) comparison between pyridine (red) and maleic acid (blue) as an internal standard.

Most of the PAAs and PNaAs investigated showed an incomplete dissolution with 5.3 to 72 % of the sample dissolved. A complete dissolution of the linear PNaA was expected due to the linear topology of the PNaA molecules; 111 % of Linear indeed dissolved in D_2O, validating our approach to quantify $\%_{diss}$. Changing the solvent from D_2O to DMSO-d_6 for different batches of NMP-tBA-1 did not affect the extent of the sample dissolution. In 1,4-dioxane-d_8 this sample's solubility was so poor that it did not even look dissolved, and this solvent was thus was not investigated further. It was also observed that changing the pD of the PNaA solution by adding NaOD did not seem to improve or change the dissolution of NMP-AA-6. No conclusive assessment on the effect of pD in NMP-AA-6 can be drawn as these samples were prepared independently at different concentrations. A possible reason for the incomplete dissolution of NMP-AA-6 in different solvents and at different pDs (as well as the incomplete dissolution of

other polymers in this work) is the presence of microgels and/or by clustering in the samples. Microgels can be formed by intermolecular chain transfer to polymer (or propagation to terminal double bonds) coupled to by termination by combination as shown for *n*-butyl acrylate.[43] Long chain branching via intermolecular chain transfer to polymer was confirmed via multiple-detection SEC in several poly(alkyl acrylates), poly(n-butyl acrylate) via RDRP[44], poly(alkyl acrylates), poly(n-butyl acrylate) via conventional radical polymerization[30, 44] and poly(2-ethylhexyl acrylate) via pulsed laser polymerization (PLP)[45]. Termination by combination has been used as a gelation technique and has been observed for methyl, and ethyl acrylates.[46] The same phenomena could possibly happen in PAAs and PNaAs investigated in this study. The incomplete solvation and clustering of PAAs with similar molecular weight in different deuterated solvents (D_2O, 1,4-dioxane-d_8, ethanol-d_6 and their mixtures) has been observed by Small-Angle Neutron Scattering (SANS) with one of the proposed reasons for the low solvation being the presence of hydrophobic end groups.[47] The clustering was proposed to be of a gel-like or network-like structure when similar clustering was observed in poly(ethylene oxide) solutions.[48] The determination of the PAA molecular weight for the SANS work may not have been accurate due to SEC calibration standards being polystyrenes[47], and different samples may have had different molecular weights. Thus, both molecular weight and end group may still influence PAA's solvation required for its dissolution. It is however clear that the distinction between soluble and insoluble in SANS and NMR does not have to be at the macromolecular level: in other words, some macromolecules might have a solvated shell and a non-solvated core. One of the implications is that the *DB* obtained by solution-state NMR may not characterize the same part of the sample as the molecular weight distribution of the soluble fraction[43, 49] determined by SEC (Figure 4).

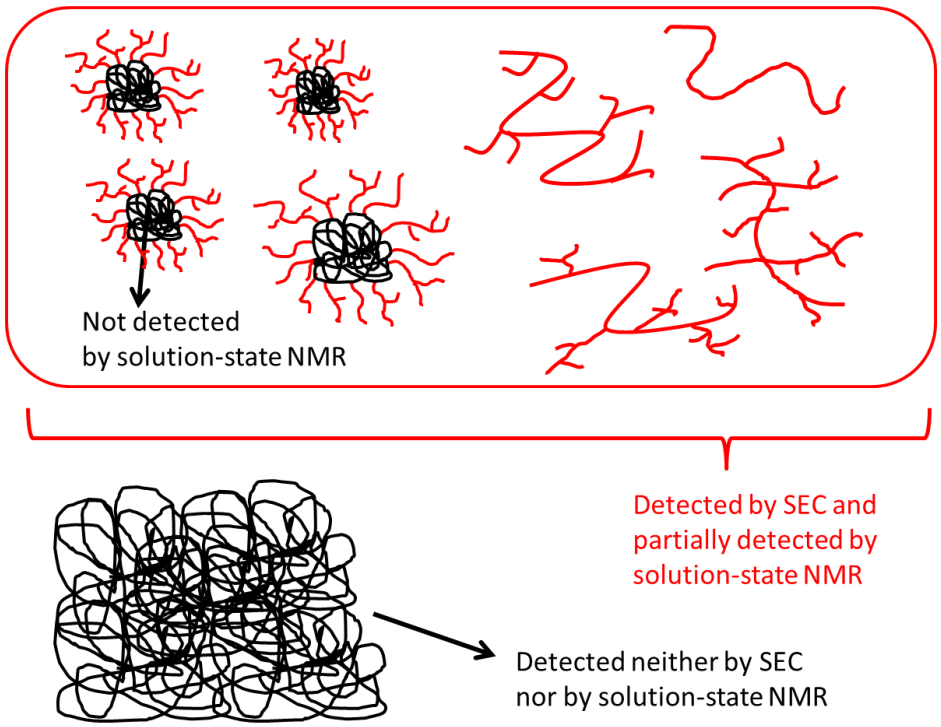

Figure 4. Schematic representation of the fractions of branched samples detected by SEC and solution-state NMR. Non-solvated sample parts, indicated in black, cannot be detected by solution-state NMR.

In the present work, some samples with the same end groups have different extents of dissolution, while some samples with different end groups exhibited similar extents of dissolution (Figure 3a). Since Linear has a considerably higher fraction dissolved than the branched samples, the presence of branching is also likely a factor influencing the solvation and clustering of PAA and PNaA. The viscosity of a sample may also influence its solubility: if its viscosity plays a role in its dissolution, its solubility will be different at different concentrations. For this study, the solubility of some PAAs and PNaAs at two different concentrations was determined: the concentrations provided in Table 2 and Table S8 and concentrations ten times lower (Figure 3b). A lower $\%_{diss}$ was observed for the diluted NMP-AA-5 in comparison to NMP-AA-5 at its original concentration. It must be noted that NMP-AA-5 and -6 were diluted only with D_2O when it should have been D_2O with NaOD. As a result, the dilution decreased the

pD which in turn made it more difficult to dissolve which explains the decreased $\%_{diss}$ for NMP-AA-5. For NMP-AA--6 in D_2O with NaOD, no significant difference in terms of solubility was observed between these two concentrations, implying that viscosity, as well as the change in pD does not influence the sample's dissolution. A higher solubility was observed for MADIX-AA-5 in the diluted sample than the concentrated sample (by a factor of ≈ 5) which suggests an influence of viscosity in the dissolution of this particular polymer when 1,4-dioxane-d_8 was used as a solvent. Thus, the influence of viscosity on *DB* quantification should be investigated for each sample as it varies from sample to sample (and solvent to solvent).

For some PAAs/PNaAs (NMP-AA-3, NMP-tBA-1 and Linear), a possible overlap between the vinylic signal of the maleic acid and the carboxylic acid signal of the polymer was detected. This would lead to an overestimate of the standard signal integral, thus to an underestimate of $\%_{diss}$. Pyridine was used as an alternative internal standard for the determination of the solubility of a few PNaAs and PAAs (Figure 3c). Higher $\%_{diss}$ values were indeed observed when pyridine was used as an internal standard for Linear and NMP-AA-6, but not for MADIX-AA-5 and -6 for which no significant difference was observed. As there was no overlap between the vinylic signal of the maleic acid and any of the signals for NMP-AA-6, MADIX-AA-5 and -6, both maleic acid and pyridine were suitable internal standards for these samples' $\%_{diss}$ determination. A significant difference in the measured $\%_{diss}$ of NMP-AA-6 was however observed with different internal standards. The dissolution of an incompletely soluble sample may not be repeatable. This stresses the importance of determining the sample's solubility for each measurement of a sample's property in solution. For future investigations, the error of the $\%_{diss}$ should be determined with pyridine as an internal standard.

Note that some of the NMR solvents used for the PAAs/PNaAs investigated in this work partially evaporated as some samples were prepared several weeks/months prior to their ^1H

NMR measurement (Figure S20). This evaporation leads to an overestimation of the $\%_{diss}$ value. This was the case for a measurement of Linear, leading to a $\%_{diss}$ of 130 ± 7 % (Figure S20). A fresh Linear sample in D_2O was thus prepared shortly before the NMR measurements (with both maleic acid and pyridine). A value of $\%_{diss}$ of about 112 ± 6 % was then observed for Linear using pyridine as an internal standard which may be due to the evaporation of the NMR solvent. Moreover, the integration of the backbone to identify the $\%_{diss}$ may sometimes include other overlapping signals (from the end group or impurities) causing further overestimations. Thus, for the assessment of the accuracy of *DB* quantification in several PAA/PNaAs, the solubility observed for most samples may sometimes be overestimated and thus actually poorer than determined in this work.

Due to the poor solubility of the samples, the accuracy of the *DB* quantification in PAA and PNaA is biased to the portion of the sample that is dissolved.

_DB_ obtained for several PAAs/PNaAs

In this work, the *DB* of several PNaAs and PAAs was quantified (Table 3). There are no significant differences between the *DB* values determined using Equations 1 and 2 (or Equations derived from them, see supporting information Equation S3 - S18). There was also no significant difference between their precision. In terms of accuracy, as mentioned earlier, full relaxation must be achieved between scans in order to ensure quantitative NMR measurements (as done in this work as well as in [24]). This is important to consider as some previous works on *DB* quantification in PAA failed proving their experimental measurements were quantitative.[21, 40]

DB values ranging from 1 to 3.5 % were obtained for most PAAs and PNaAs. It must however be acknowledged that only the soluble portion of the sample was quantified. The *DB* is one of the soluble fraction only, which may be different from the *DB* of the whole sample. The

insoluble fraction may have a higher incidence of long branches than the soluble fraction, or even crosslinking; the soluble fraction may have a higher incidence of short branches than the insoluble fraction. It is thus impossible to predict whether the average *DB* of the soluble fraction in that specific solvent would underestimate or overestimate the *DB* of the whole sample. Both the absence of significant differences[49] between the soluble fraction and the whole sample, and a lower *DB* value for the soluble fraction[49] have been observed for hydrophobic polyacrylates. The assessment of the solubility of PAAs/PNaAs is therefore an important contribution to the assessment of the accuracy of their *DB* quantification. Note that previous works failed to acknowledge the fact that the *DB* quantified may not represent the whole PAA sample.[20, 21, 40]The determination of kinetic coefficients, such as the backbiting one[24, 40], from *DB* is done on the assumption that the full sample is analyzed. Determination of the solubility of these samples will allow to determine the accuracy of the backbiting rate coefficients.

Table 3. Average *DB* of several PAAs/PNaAs quantified through the signals from the backbone (Equation 1 or one of its derivatives) or the carboxylic acid group (Equation 2 or one of its derivatives). NMP-AA-6 displayed a C_q signal below detection limit and thus its *DB* was not quantified.

Sample	**Integration range of C_q signal (ppm)**	***DB* (%) backbone**	***DB* (%) *COOH***
NMP-AA-1	46.7 - 50.0	3.1 ± 0.2	3.1 ± 0.2
NMP-AA-3	46.5 - 50.9	3.3 ± 0.2	3.4 ± 0.2
NMP-AA-5 with NaOD	49.5 – 53.2	2.0 ± 0.6	2.1 ± 0.7
MADIX-AA-4	46.5 – 49.6	2.4 ± 0.2	2.3 ± 0.1
MADIX-AA-5	47.0 – 49.5	2.3 ± 0.2	2.3 ± 0.2
MADIX-AA-6	47.0 – 49.7	3.3 ± 0.2	3.3 ± 0.2
ATRP-tBA-1[a]	46.5-50.1	1.6 ± 0.3	1.7 ± 0.3
ATRP-tBA-2[a]	46.4-49.3	1.1 ± 0.1	1.1 ± 0.2
Conv-AA-1	46.3-50.0	2.6 ± 0.2	2.6 ± 0.2

[a]DB is an overestimated value because of a possible overlap between GN V and GN 17 (GN17 not taken into account in the DB quantification).

CONCLUSION

Several parameters that could influence the precision and the accuracy of the *DB* quantification in PAAs/PNaAs were investigated in this work. Most PAAs and PNaAs exhibited incomplete dissolution resulting in a determined *DB* not representative of the whole sample. This is a major issue in terms of accuracy of the *DB* values. Thus, it might be worth considering *DB* quantification in PAAs/PNaAs using swollen-state NMR spectroscopy despite its poor resolution

in future investigations. Better solvation of PAA in mixed solvents was observed in comparison to individual solvents.[47] *DB* quantification of PAA dissolved in mixed solvents will be investigated in the future.

The error introduced during data treatment was also estimated to assess the precision of *DB* quantification. An empirical equation was derived to take into account the error originating in both the limited signal-to-noise ratio and the user-dependent data treatment.

With the knowledge obtained in this work the precision and accuracy of the *DB* quantification of PAAs/PNaAs can be assessed. With these factors taken into account, PAA/PNaA samples can be compared in terms of their average *DB*. This will shed light on the different levels of branching obtained with various polymerization pathways, enabling the intelligent design of the polymers for advanced applications. An accurate determination of the average *DB* is also needed if one wants to understand and predict functional properties, such as mechanical or adhesive properties. The current values of *DB* of soluble fractions should be relevant to understand properties in solution such as binding (flocculation or drug binding).

ASSOCIATED CONTENT

Supporting Information

The Supporting Information is available free of charge via the ACS publication website (http://pubs.acs.org).

Estimation of T_1 for quantitative measurements,^{13}C NMR spectra with full NMR signal assignments, modified equations for *DB* quantification, information on dissolution studies (*PNR* calculation and precision, ^{1}H NMR with partial signal assignment, TGA) are shown in the Supporting Information.

ACKNOWLEDGMENT

Many thanks to Kevin Dizon, Aaron Rebmann and Michael Horgan (WSU) for their participation in round robin tests for data treatment. AM would also like to thank Dr Joel Thevarajah for being a participant in round robin tests for data treatment as well as his contribution in scientific discussions. AM would like to thank Dr Timothy Murphy and the Advanced Materials Characterisation Facility (AMCF) at WSU for assistance with the TGA. AM and AS acknowledge the Australian Commonwealth government for their Australian Postgraduate Awards (APA) scholarship and a RTP scholarship respectively. Many thanks to Dr Yohann Guillaneuf, Dr Catherine Lefay, Dr Ihor Kulai, Dr Simon Harrisson, Prof. Mathias Destarac and Assoc. Prof. Christopher M. Fellows for their contribution to synthesis and fruitful scientific discussions.

REFERENCES

1. Gaborieau, M.; Castignolles, P. Size-exclusion chromatography (SEC) of branched polymers and polysaccharides, *Analytical and Bioanalytical Chemistry* **2011,** 399, 1413-1423.
2. Kim, J.; Kim, D. H.; Son, Y. Rheological properties of long chain branched polyethylene melts at high shear rate, *Polymer* **2009,** 50, 4998-5001.
3. Wang, L.; Hu, P.; Tirelli, N. Amphiphilic star block copolymers: Influence of branching on lyotropic/interfacial properties, *Polymer* **2009,** 50, 2863-2873.
4. Buchholtz, F. L., Polyacrylamides and Poly(Acrylic Acids). In *Ullmann´s Encyclopedia of Industrial Chemistry*, 7th ed.; Wiley-VCH: Weinheim, Germany, 2000; Vol. A21.
5. Ratnapandian, S.; Warner, S. B. Modern diaper technology, *Tappi Journal* **1996,** 79, 173-177.
6. Yu, Y.; Peng, R. G.; Yang, C.; Tang, Y. H. Eco-friendly and cost-effective superabsorbent sodium polyacrylate composites for environmental remediation, *Journal of Materials Science* **2015,** 50, 5799-5808.
7. Yuk, S. H.; Cho, S. H.; Lee, H. B. Electric current-sensitive drug delivery systems using sodium alginate poly(acrylic acid) composites *Pharmaceutical Research* **1992,** 9, 955-957.
8. Thaurer, M. H.; Deutel, B.; Schlocker, W.; Bernkop-Schnurch, A. Development of nanoparticulate drug delivery systems based on thiolated poly(acrylic acid), *Journal of Microencapsulation* **2009,** 26, 187-194.
9. Perera, G.; Greindl, M.; Palmberger, T. F.; Bernkop-Schnurch, A. Insulin-loaded poly(acrylic acid)-cysteine nanoparticles: Stability studies towards digestive enzymes of the intestine, *Drug Delivery* **2009,** 16, 254-260.

10. Kriwet, B.; Walter, E.; Kissel, T. Synthesis of bioadhesive poly(acrylic acid) nano- and microparticles using an inverse emulsion polymerization method for the entrapment of hydrophilic drug candidates, *Journal of Controlled Release* **1998,** 56, 149-158.
11. De, T. K.; Hoffman, A. S. A reverse microemulsion polymerization method for preparation of bioadhesive polyacrylic acid nanoparticles for mucosal drug delivery: Loading and release of timolol maleate, *Artificial Cells Blood Substitutes and Immobilization Biotechnology* **2001,** 29, 31-46.
12. Cui, D. C.; Lu, W. L.; Sa, E. A.; Gu, M. J.; Lu, X. J.; Fan, T. Y. Poly(acrylic acid) microspheres loaded with lidocaine: Preparation and characterization for arterial embolization, *International Journal of Pharmaceutics* **2012,** 436, 527-535.
13. Whitty, E. G., Maniego, A. R., Bentwitch, S. A., Guillaneuf, Y., Jones, M. R., Gaborieau, M., Castignolles, P. Cellular response to linear and branched poly(acrylic acid), *Macromolecular Bioscience* **2015,** 15, 1724-1734.
14. Dai, Y.; Zhang, C.; Cheng, Z.; Ma, P. a.; Li, C.; Kang, X.; Yang, D.; Lin, J. pH-responsive drug delivery system based on luminescent CaF2:Ce3+/Tb3+-poly(acrylic acid) hybrid microspheres, *Biomaterials* **2012,** 33, 2583-2592.
15. Huang, Y. H.; Yu, H. Q.; Xiao, C. B. pH-sensitive cationic guar gum/poly (acrylic acid) polyelectrolyte hydrogels: Swelling and in vitro drug release, *Carbohydrate Polymers* **2007,** 69, 774-783.
16. East, C. P.; Wallace, A. D.; Al-Hamzah, A.; Doherty, W. O. S.; Fellows, C. M. Effect of Poly(acrylic acid) Molecular Mass and End-Group Functionality on Calcium Oxalate Crystal Morphology and Growth, *Journal of Applied Polymer Science* **2010,** 115, 2127-2135.
17. Wallace, A. D.; Al-Hamzah, A.; East, C. P.; Doherty, W. O. S.; Fellows, C. M. Effect of Poly(acrylic acid) End-Group Functionality on Inhibition of Calcium Oxalate Crystal Growth, *Journal of Applied Polymer Science* **2010,** 116, 1165-1171.
18. Taton, D.; Wilczewska, A. Z.; Destarac, M. Direct synthesis of double hydrophilic statistical di- and triblock copolymers comprised of acrylamide and acrylic acid units via the MADIX process, *Macromolecular Rapid Communications* **2001,** 22, 1497-1503.
19. Al-Hamzah, A. A.; Smith, E. J.; Fellows, C. M. Inhibition of Homogeneous Formation of Magnesium Hydroxide by Low-Molar-Mass Poly(acrylic acid) with Different End-Groups, *Industrial & Engineering Chemistry Research* **2015,** 54, 2201-2207.
20. Loiseau, J.; Doerr, N.; Suau, J. M.; Egraz, J. B.; Llauro, M. F.; Ladaviere, C. Synthesis and characterization of poly(acrylic acid) produced by RAFT polymerization. Application as a very efficient dispersant of $CaCO_3$, kaolin, and TiO_2, *Macromolecules* **2003,** 36, 3066-3077.
21. Couvreur, L.; Lefay, C.; Belleney, J.; Charleux, B.; Guerret, O.; Magnet, S. First Nitroxide-Mediated Controlled Free-Radical Polymerization of Acrylic Acid, *Macromolecules* **2003,** 36, 8260-8267.
22. Maniego, A. R.; Ang, D.; Guillaneuf, Y.; Lefay, C.; Gigmes, D.; Aldrich-Wright, J. R.; Gaborieau, M.; Castignolles, P. Separation of poly(acrylic acid) salts according to the topology using capillary electrophoresis in the critical conditions, *Analytical and Bioanalytical Chemistry* **2013,** 405, 9009-9020.
23. Lacík, I.; Stach, M.; Kasák, P.; Semak, V.; Uhelská, L.; Chovancová, A.; Reinhold, G.; Kilz, P.; Delaittre, G.; Charleux, B.; Chaduc, I.; D'Agosto, F.; Lansalot, M.; Gaborieau, M.; Castignolles, P.; Gilbert, R. G.; Szablan, Z.; Barner-Kowollik, C.; Hesse, P.; Buback, M. SEC Analysis of Poly(Acrylic Acid) and Poly(Methacrylic Acid), *Macromolecular Chemistry and Physics* **2015,** 216, 23-37.

24. Lena, J.-B.; Goroncy, A. K.; Thevarajah, J. J.; Maniego, A. R.; Russell, G. T.; Castignolles, P.; Gaborieau, M. Effect of transfer agent, temperature and initial monomer concentration on branching in poly(acrylic acid): A study by 13C NMR spectroscopy and capillary electrophoresis, *Polymer* **2017,** 114, 209-220.
25. Striegel, A. M.; Krejsa, M. R. Complementarity of universal calibration SEC and C-13 NMR in determining the branching state of polyethylene, *Journal of Polymer Science Part B Polymer Physics* **2000,** 38, 3120-3135.
26. Klimke, K.; Parkinson, M.; Piel, C.; Kaminsky, W.; Spiess, H. W.; Wilhelm, M. Optimisation and application of polyolefin branch quantification by melt-state C-13 NMR spectroscopy, *Macromolecular Chemistry and Physics* **2006,** 207, 382-395.
27. Ahmad, N. M.; Heatley, F.; Lovell, P. A. Chain transfer to polymer in free-radical solution polymerization of n-butyl acrylate studied by NMR spectroscopy, *Macromolecules* **1998,** 31, 2822-2827.
28. Plessis, C.; Arzamendi, G.; Alberdi, J. M.; Agnely, M.; Leiza, J. R.; Asua, J. M. Intramolecular chain transfer to polymer in the emulsion polymerization of 2-ethylhexyl acrylate, *Macromolecules* **2001,** 34, 6138-6143.
29. Ahmad, N. M.; Charleux, B.; Farcet, C.; Ferguson, C. J.; Gaynor, S. G.; Hawkett, B. S.; Heatley, F.; Klumperman, B.; Konkolewicz, D.; Lovell, P. A.; Matyjaszewski, K.; Venkatesh, R. Chain Transfer to Polymer and Branching in Controlled Radical Polymerizations of n-Butyl Acrylate, *Macromolecular Rapid Communications* **2009,** 30, 2002-2021.
30. Castignolles, P.; Graf, R.; Parkinson, M.; Wilhelm, M.; Gaborieau, M. Detection and quantification of branching in polyacrylates by size-exclusion chromatography (SEC) and melt-state 13C NMR spectroscopy, *Polymer* **2009,** 50, 2373-2383.
31. Gaborieau, M.; Koo, S. P. S.; Castignolles, P.; Junkers, T.; Barner-Kowollik, C. Reducing the degree of branching in polyacrylates via midchain radical patching: a quantitative melt-state NMR study, *Macromolecules* **2010,** 43, 5492–5495.
32. Qiu, X. H.; Zhou, Z.; Gobbi, G.; Redwine, O. D. Error Analysis for NMR Polymer Microstructure Measurement without Calibration Standards, *Analytical Chemistry* **2009,** 81, 8585-8589.
33. Klimke, K.; Parkinson, M.; Piel, C.; Kaminsky, W.; Spiess, H. W.; Wilhelm, M. Optimisation and Application of Polyolefin Branch Quantification by Melt-State 13C NMR Spectroscopy, *Macromolecular Chemistry and Physics* **2006,** 207, 382-395.
34. Klimke, K. Optimised polyolefin branch quantification by ^{13}C NMR spectroscopy. PhD thesis, Johannes Gutenberg Universitaet Mainz, Germany, 2006. http://ubm.opus.hbz-nrw.de/volltexte/2006/1077/
35. Thevarajah, J. J.; Bulanadi, J. C.; Wagner, M.; Gaborieau, M.; Castignolles, P. Towards a less biased dissolution of chitosan, *Analytica Chimica Acta* **2016,** 935, 258 - 268.
36. McNeill, I. C.; Sadeghi, S. M. T. Thermal-stability and degradation mechanisms of poly(acylic acid) and its salts. 1. Poly(acrylic acid), *Polymer Degradation and Stability* **1990,** 29, 233-246.
37. Caykara, T.; Guven, O. Effect of preparation methods on thermal properties of poly(acrylic acid) silica composites, *Journal of Applied Polymer Science* **1998,** 70, 891-895.
38. Sutton, A. T.; Read, E.; Maniego, A. R.; Thevarajah, J. J.; Marty, J.-D.; Destarac, M.; Gaborieau, M.; Castignolles, P. Purity of double hydrophilic block copolymers revealed by capillary electrophoresis in the critical conditions, *Journal of Chromatography A* **2014,** 1372, 187-195.

39. Gottlieb, H. E.; Kotlyar, V.; Nudelman, A. NMR chemical shifts of common laboratory solvents as trace impurities, *Journal of Organic Chemistry* **1997,** 62, 7512-7515.
40. Wittenberg, N. F. G.; Preusser, C.; Kattner, H.; Stach, M.; Lacík, I.; Hutchinson, R. A.; Buback, M. Modeling Acrylic Acid Radical Polymerization in Aqueous Solution, *Macromolecular Reaction Engineering* **2015,** 10, 95-107.
41. Schmitz, S.; Dona, A. C.; Castignolles, P.; Gilbert, R. G.; Gaborieau, M. Assessment of the Extent of Starch Dissolution in Dimethyl Sulfoxide by 1H NMR Spectroscopy, *Macromolecular Bioscience* **2009,** 9, 506-514.
42. Fujita, M.; Iizuka, Y.; Miyake, A. Thermal and kinetic analyses on Michael addition reaction of acrylic acid, *Journal of Thermal Analysis and Calorimetry* **2016**, 1-7.
43. Plessis, C.; Arzamendi, G.; Leiza, J. R.; Schoonbrood, H. A. S.; Charmot, D.; Asua, J. M. Seeded semibatch emulsion polymerization of n-butyl acrylate. Kinetics and structural properties, *Macromolecules* **2000,** 33, 5041-5047.
44. Gaborieau, M.; Nicolas, J.; Save, M.; Charleux, B.; Vairon, J.-P.; Gilbert, R. G.; Castignolles, P. Multiple-detection size-exclusion chromatography of complex branched polyacrylates, *Journal of Chromatography A* **2008,** 1190, 215-233.
45. Castignolles, P. Transfer to Polymer and Long-Chain Branching in PLP-SEC of Acrylates, *Macromolecular Rapid Communications* **2009,** 30, 1995 - 2001.
46. Bamford, C. H.; Dyson, R. W.; Eastmond, G. C. Network formation. 4. Nature of termination reaction in free-radical polymerization *Polymer* **1969,** 10, 885-889.
47. Hammouda, B.; Horkay, F.; Becker, M. L. Clustering and solvation in poly(acrylic acid) polyelectrolyte solutions, *Macromolecules* **2005,** 38, 2019-2021.
48. Hammouda, B.; Ho, D. L.; Kline, S. Insight into clustering in poly(ethylene oxide) solutions, *Macromolecules* **2004,** 37, 6932-6937.
49. Agirre, A.; Santos, J. I.; Leiza, J. R. Toward Understanding the Architecture (Branching and MWD) of Crosslinked Acrylic Latexes, *Macromolecular Chemistry and Physics* **2013,** 214, 589-598.

Supporting Information for

Assessment of the branching quantification in poly(acrylic acid): is it as easy as it seems?

Alison R. Maniego[1,2], Adam T. Sutton[1,2]†, Marianne Gaborieau[1,2],Patrice Castignolles[2]*

[1]Western Sydney University, Medical Sciences Research Group, Parramatta, Australia

[2]Western Sydney University, Australian Centre for Research on Separation Sciences (ACROSS), School of Science and Health (SSH), Parramatta, Australia

† Present address: AS Future Industries Institute (FII), University of South Australia, Mawson Lakes, South Australia 5011, Australia

* corresponding author: m.gaborieau@westernsydney.edu.au

Table of Contents

Polymer synthesis

The synthesis and SEC conditions were similar to published ones for samples synthesized with NMP[1], conventional radical polymerization[1], MADIX[2], and ATRP[3, 4]. PAAs/PNaAs were obtained by NMP from the polymerization of acrylic acid (or *t*-butyl acrylate) using the initiator of choice (provided in Table 1) in dioxane (except for NMP-AA-5 and -6, which were synthesized in water) at 90 – 120 °C. PAAs/PNaAs were obtained by conventional radical polymerization from acrylic acid, using 2,2'-azobisisobutyronitrile (AIBN) in dioxane at 80 °C. PAAs/PNaAs were obtained by MADIX from acrylic acid, using the chosen initiator (provided in Table 1) and Rhodixan A1 as chain transfer agent in dioxane at 90 – 110 °C. PAAs/PNaAs were obtained by ATRP from *t*-butyl acrylate, using the initiator of choice (provided in Table 1) in tetrahydrofuran at 90 °C; the resulting poly(*t*-butyl acrylate) was hydrolyzed using trifluoroacetic acid to yield PAA. A linear PNaA sample was purchased from Polymer Standard Service (Mainz, Germany, lot number paa26027).

Estimation of longitudinal relaxation times T_1

In NMR spectroscopy, perturbation of nuclear spins occurs when a radio frequency pulse acts on a sample, creating a measurable magnetization but also causing an imbalance of the thermal equilibrium.[5] The measurable magnetization eventually decreases which leads to the re-establishment of thermal equilibrium. This phenomenon is called the longitudinal relaxation.[5] The resolution and sensitivity of NMR spectra can thus be influenced by relaxation rates.[5] In particular, relative ratios of individual signals are affected by incomplete relaxation.

NMR procedures were managed with care in order to determine the true relative signal integrals. The repetition times between scans are set to at least five times the longitudinal

relaxation time ($5T_1$) for all signals of interest to enable their complete recovery between scans and ensure that the recorded spectra are quantitative.

Several one-dimensional inversion-recovery T_1 relaxation measurements (1D T_1) were conducted to determine which parameters would enable full relaxation between scans in order for all signals of interest to be quantitative.[5] Each 1D T_1 has a single delay τ in the "indirect dimension", and corresponding repetition delays of 5 × 1.44 times that value. In 1D T_1 tests, negative signals are observed for short τ delay values, positive ones for long τ delay values, and a zero crossing occurring at T_1/1.44.

For ^{13}C NMR spectra of the PAA samples, the tested T_1 values ranged from 1 to 4 s. For example, between τ values of 1×1.44 s and 1.2×1.44s, one signal of interest (quaternary carbon, Cq, backbone) changed from about zero to positive for NMP-AA-1 (Figure S1). This therefore shows that the T_1 value for this signal is higher than 1 s and lower than 1.2 s. Consequently a ^{13}C NMR spectrum recorded with 5 × 1.2 = 6 s will exhibit a quantitative C_q signal. It should be noted that 1.2 s is an overestimate of the T_1 for all signals of interest in most PAA samples unless indicated otherwise (see Table 2 of main manuscript).

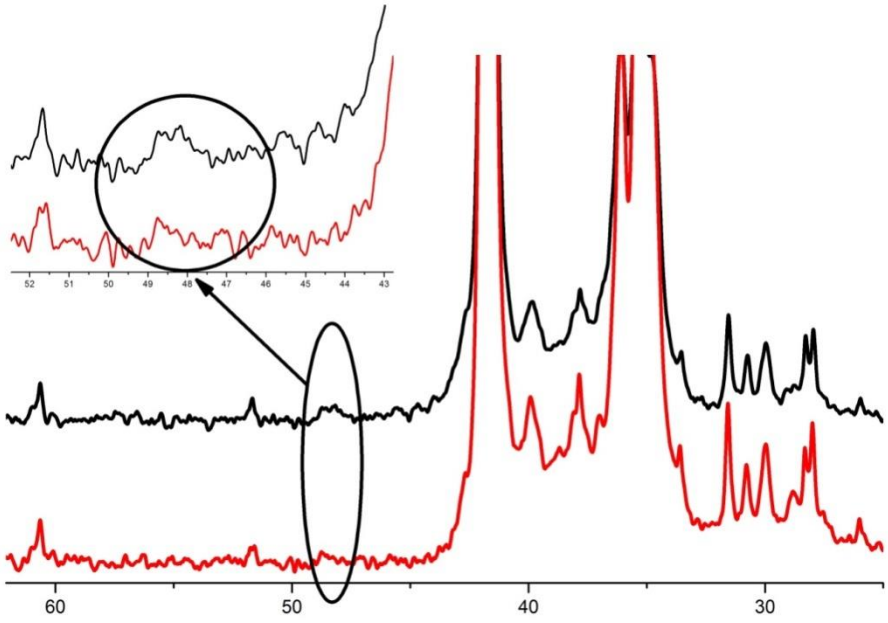

Figure S1. Estimation of T_1 of NMP-AA-1 using the one-dimensional inversion recovery pulse sequence testing for T_1values of 1.2 s with 8,248 scans over 15 h and 44 min (black) and of 1 s with 10,960 scans over 17 h and 27 min (red). Insert shows the C_q signal from the branching point.

Estimate of the error in RSD_{SNR}

Deriving Equation 3 against SNR results in:

$$\frac{d(RSD_{\mathrm{SNR}})}{dSNR} = \frac{238}{SNR^{2.28}} \tag{S1}$$

$$d(RSD_{\mathrm{SNR}}) = \frac{238 \times dSNR}{SNR^{2.28}} \tag{S2}$$

Representative ^{13}C NMR spectra of PAAs and PNaAs

PAAs/PNaAs obtained by conventional and reversible-deactivation radical polymerization were measured using 13C NMR spectroscopy. A DEPT-135 spectrum was recorded to help with the signal assignment. In DEPT-135, CH- and CH3 signals are positive whilst CH2 signals are negative. The quaternary carbon shows no signal which helps confirm the suspected Cq branching signal. Selected 13C NMR spectra of PAA/PNaA are shown as representative spectra for all samples investigated for this study.CONV-AA-1, NMP-AA-1, -3, -4, -5 and -6, ATRP-tBA-1 and -2, MADIX-AA-4, -5 and -6 were measured and their signals assigned (Table S1 – S7).

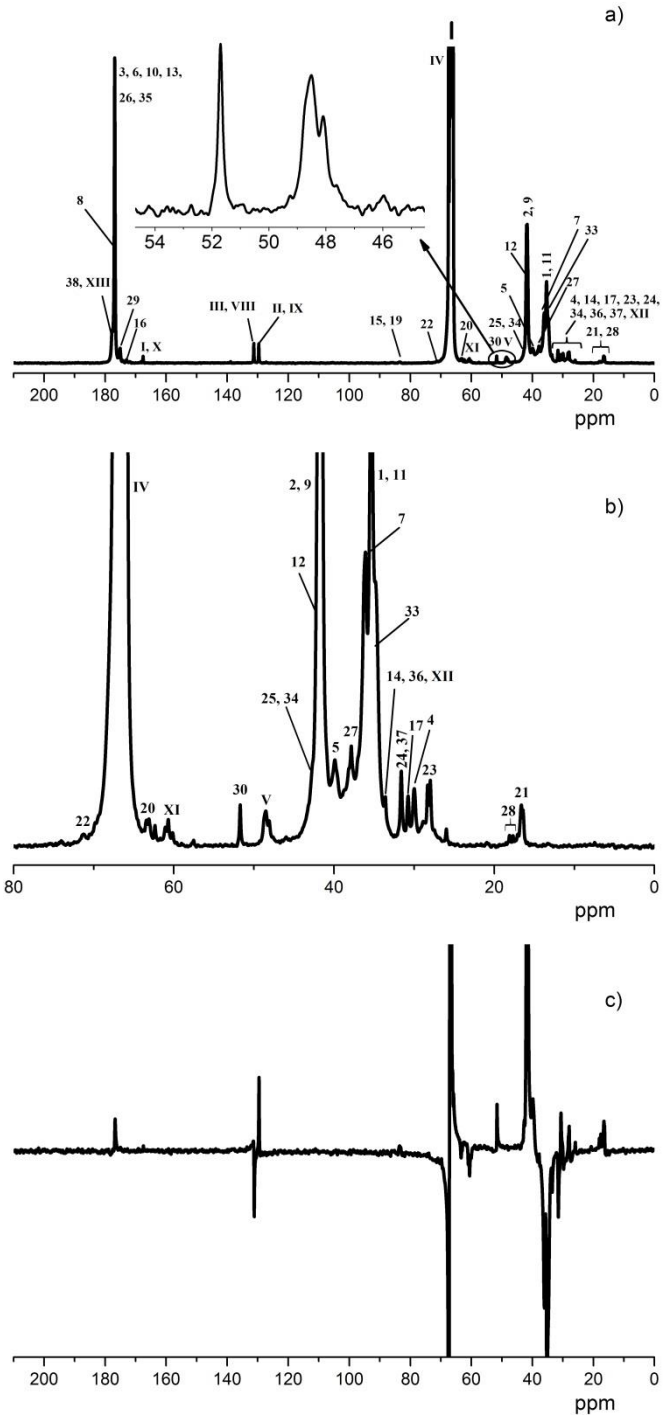

Figure S2. Solution-state ^{13}C NMR spectra of NMP-AA-1 (75.48 MHz, 1,4-dioxane-d_8): a) full quantitative spectrum with insert showing the region of the C_q signal of the branching point, b) 0 to 80 ppm region of quantitative ^{13}C NMR spectrum and c) DEPT-135 spectrum. See Figure S12, S13a, S14a and S14c for the chemical structure and Table S1 for signal assignments.

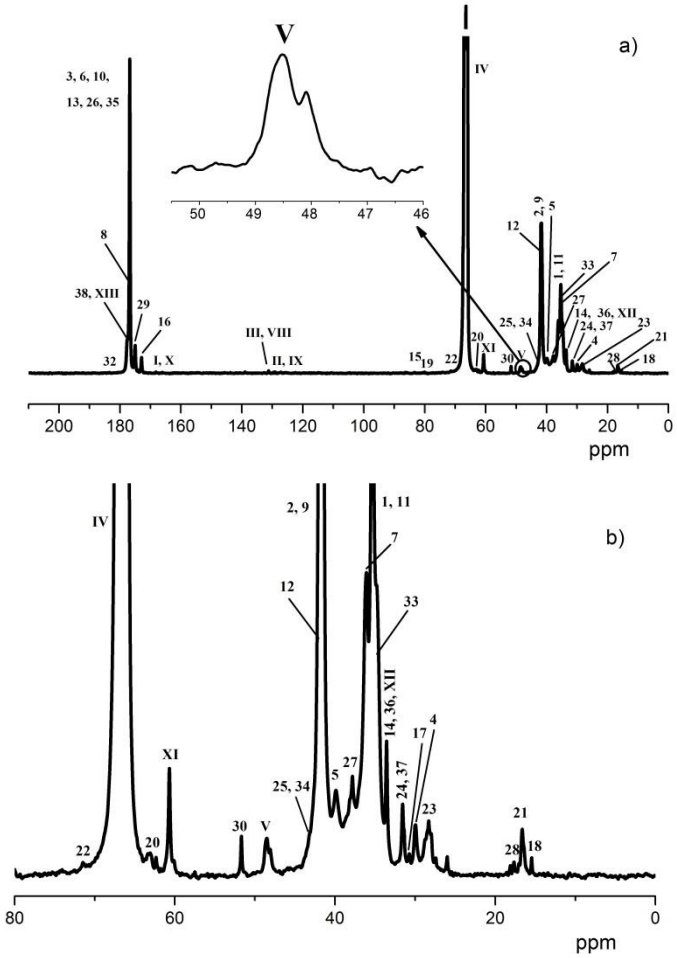

Figure S3. Solution-state ^{13}C NMR spectrum of NMP-AA-3 (75.48 MHz, 1,4-dioxane-d_8): a) full quantitative spectrum with insert showing the region of the C_q signal of the branching point and b) 0 to 80 ppm region of quantitative ^{13}C NMR spectrum. See Figure S12, S13b, S14a, and S14c for the chemical structure and Table S1 for signal assignment.

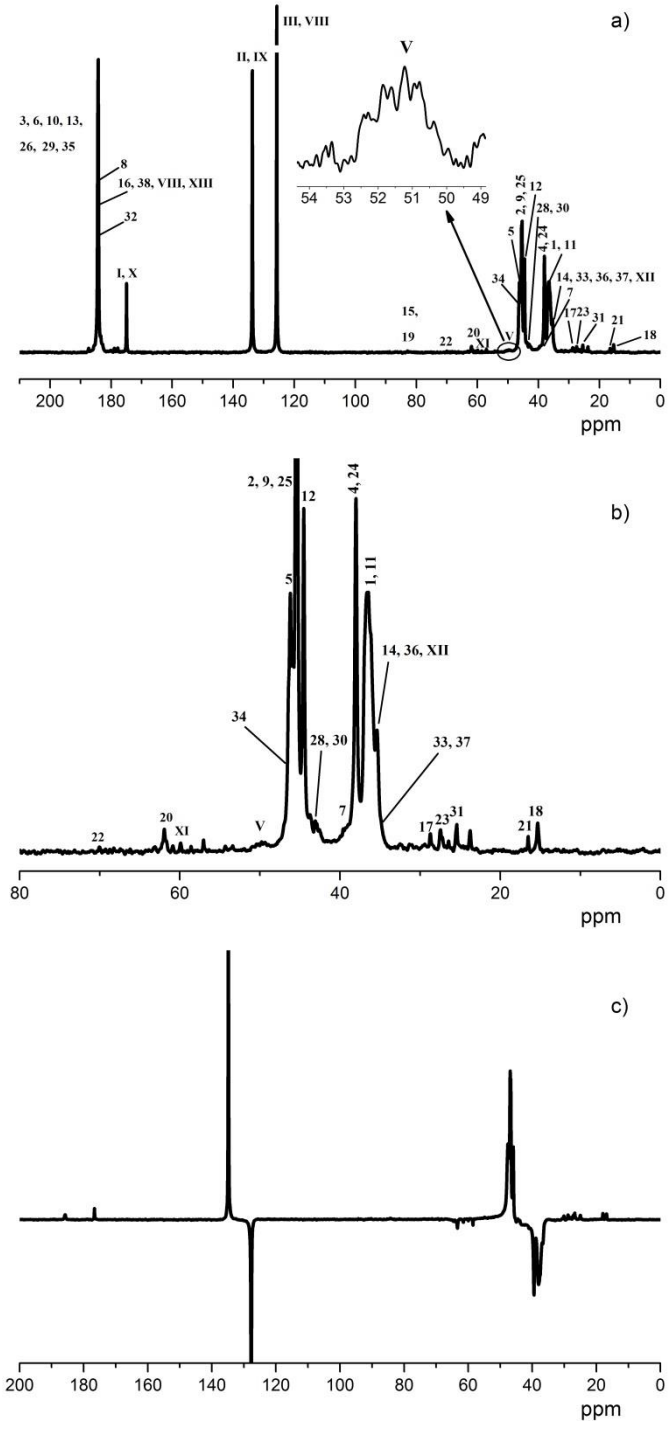

Figure S4. Solution-state ^{13}C NMR spectra of NMP-AA-5 (75 MHz, D_2O): a) full quantitative spectrum with insert showing the region of the C_q signal of the branching point, b) 0 to 60 ppm region of quantitative ^{13}C NMR spectrum and c) DEPT-135 spectrum. See Figure S12, S13b, S14a and S14c for the chemical structure and Table S2 for signal assignment

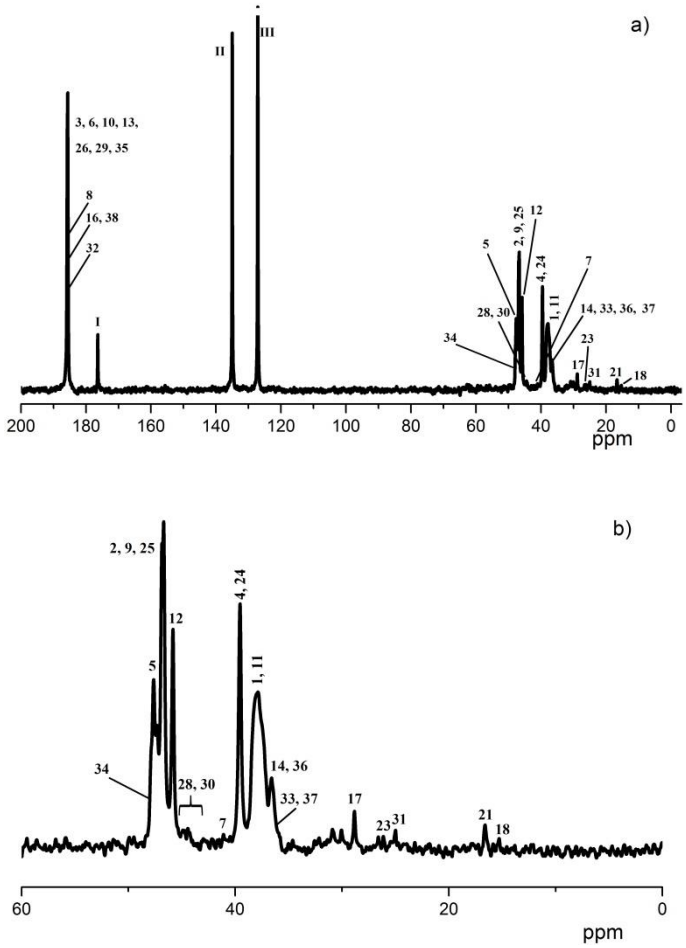

Figure S5. Solution-state ^{13}C NMR spectrum of NMP-AA-6 (75.48 MHz, D_2O): a) full quantitative spectrum with the C_q branching signal below the detection limit and b) 0 to 60 ppm region of quantitative ^{13}C NMR spectrum. See Figure S12, S13b, S14a and S14c for the chemical structure and Table S2 for signal assignment.

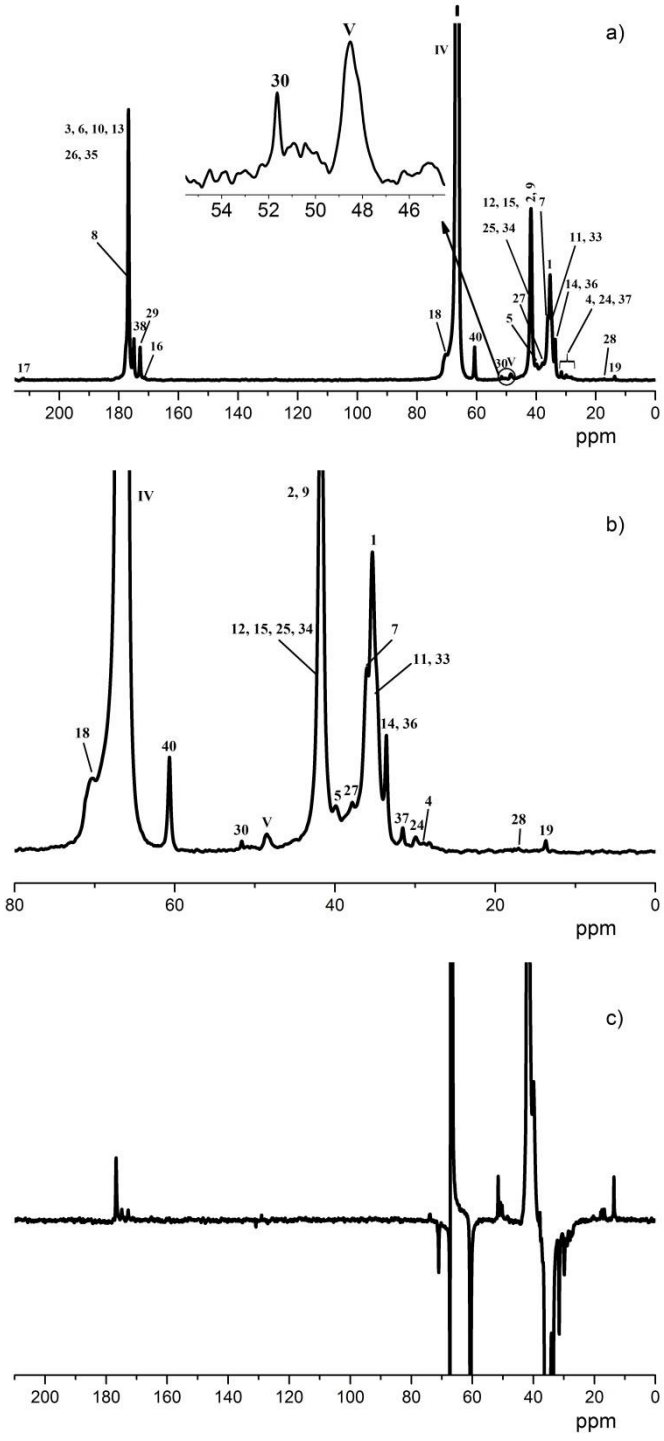

Figure S6. Solution-state ^{13}C NMR spectra of MADIX-AA-5 (75.48 MHz, 1,4-dioxane-d_8): a) full quantitative spectrum with insert showing the region of the C_q signal of the branching point, b) 0 to 80 ppm region of quantitative ^{13}C NMR spectrum and c) DEPT-135 spectrum. See Figure S12, S13a, S14b and S14c for the chemical structure and Table S3 for the signal assignment.

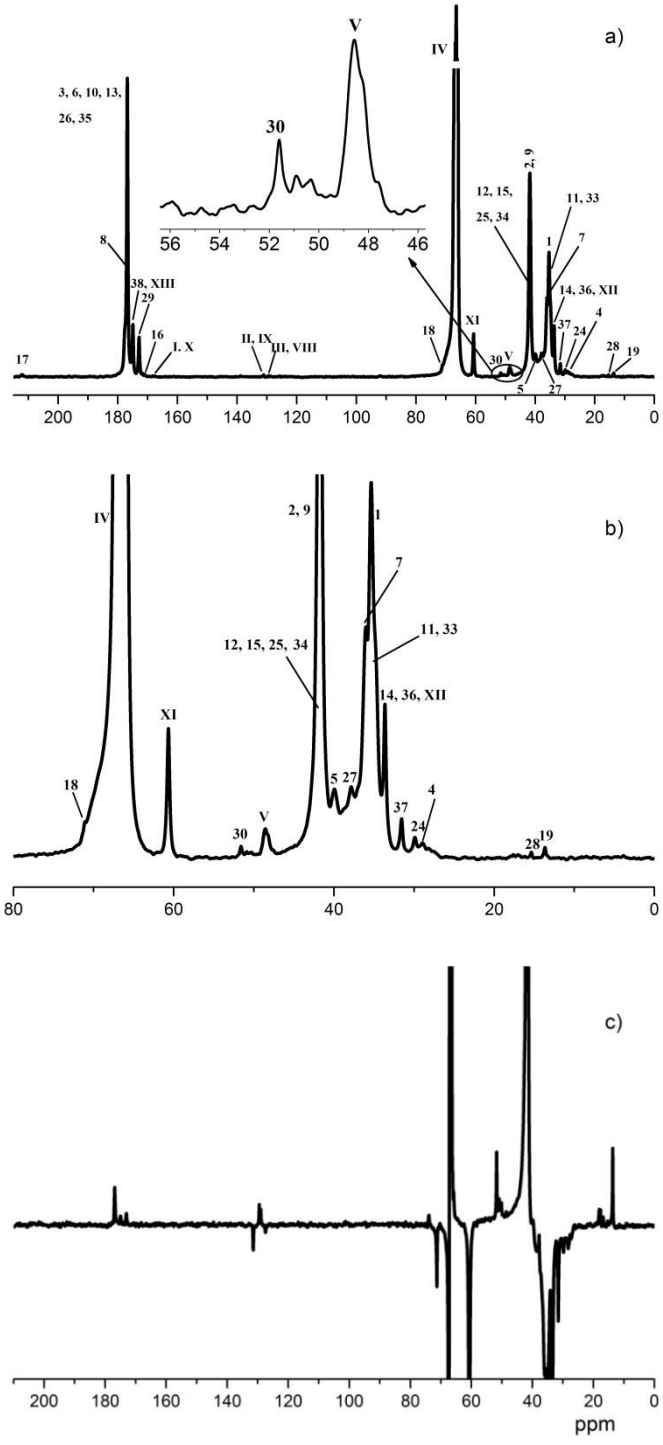

Figure S7. Solution-state ^{13}C NMR spectra of MADIX-AA-6 (75.48 MHz, 1,4-dioxane-d_8): a) full quantitative spectrum with insert showing the region of the C_q signal of the branching point, b) 0 to 80 ppm region of quantitative ^{13}C NMR spectrum and c) DEPT-135 spectrum. See Figure S12, S13a, S14b and S14c for the chemical structure and Table S3 for the signal assignment.

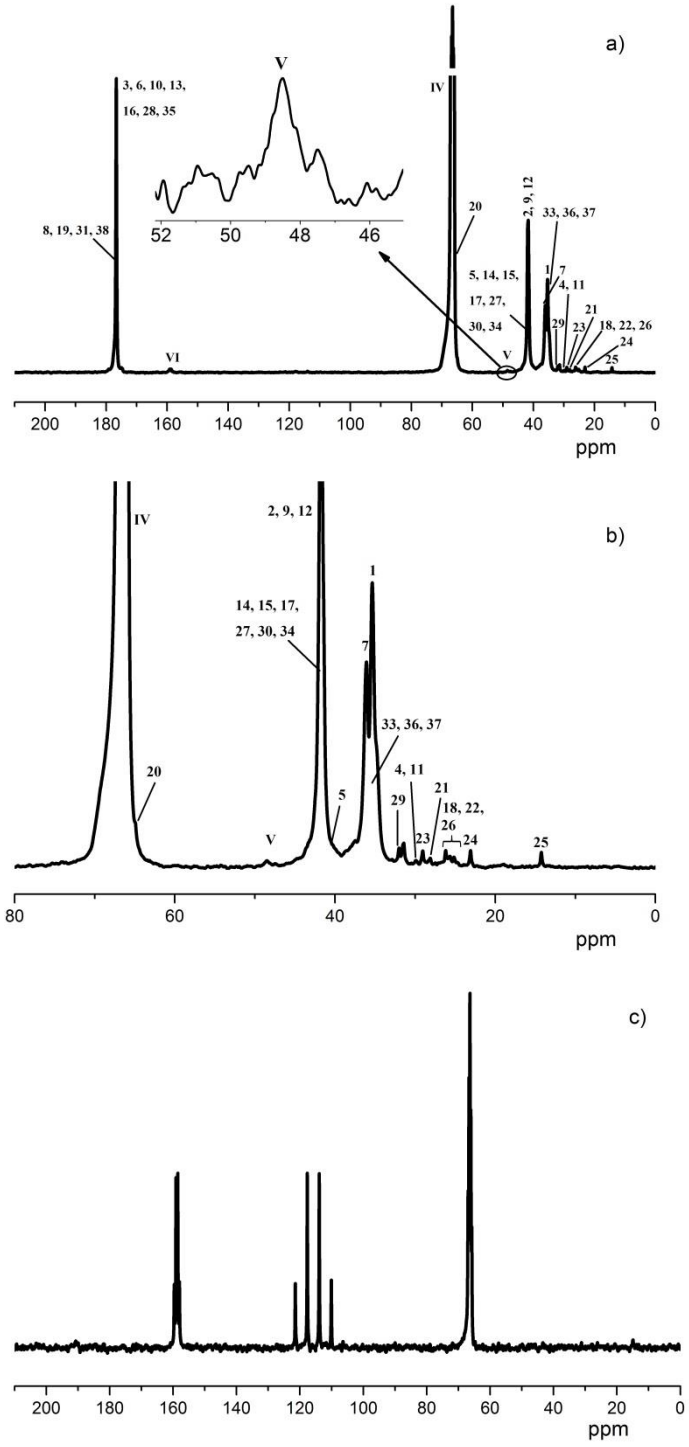

Figure S8. Solution-state ^{13}C NMR spectrum of ATRP-tBA-1 (75.48 MHz, 1,4-dioxane-d_8): a) full quantitative spectrum with insert showing the region of the C_q signal of the branching point, b) 0 to 80 ppm region of quantitative ^{13}C NMR spectrum and c) full quantitative spectrum of trifluoroacetic acid (TFA) in 1,4-dioxane-d_8, used to confirm signal VI. See Figure S12, S13c, S14c, S14d and S14e for the chemical structure and Table S4 for signal assignment.

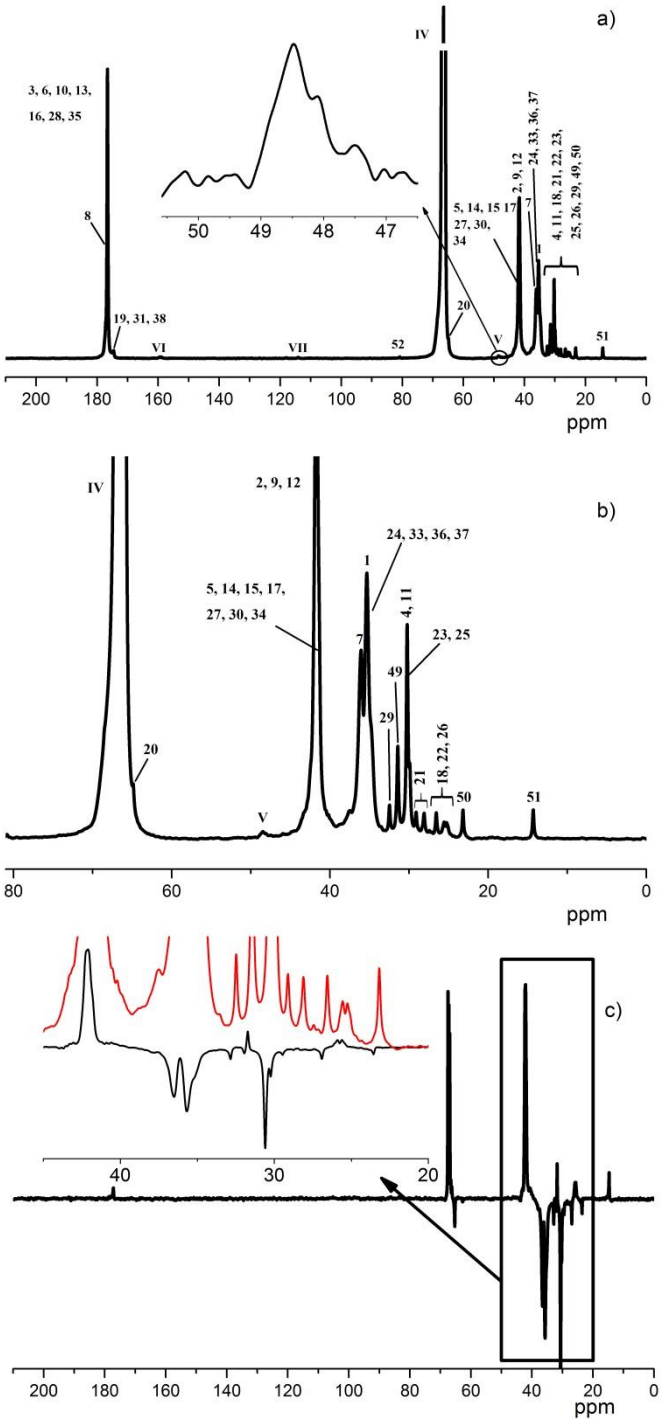

Figure S9. Solution-state ^{13}C NMR spectra of ATRP-tBA-2 (75.48 MHz, 1,4-dioxane-d_8) with: a) full quantitative spectrum with insert showing the region of the C_q signal of the branching point, b) 0 to 80 ppm region of quantitative ^{13}C NMR spectrum and c) DEPT-135 spectrum with zoom insert of the DEPT-135 spectrum (black) overlaid with the quantitative

^{13}C spectrum (red) from 20 to 50 ppm. See Figure S12, S13d, S14c, and S14e for the chemical structure and Table S5 for signal assignment.

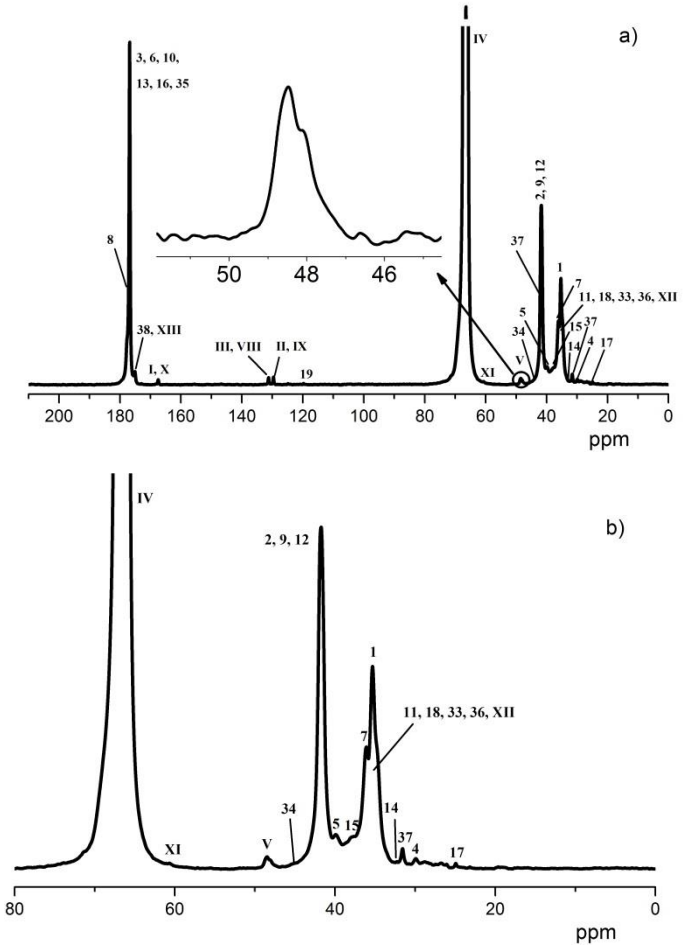

Figure S10.Solution-state ^{13}C NMR spectra of CONV-AA-1 (75.48 MHz, 1,4-dioxane-d_8):a) full quantitative spectrum and b) 0 to 80 ppm region of quantitative ^{13}C NMR spectrum. See Figure S12, S13e and S14c for the chemical structure and Table S6 for signal assignment.

^{13}C NMR signal assignment

The full signal assignment for PAAs/PNaAs measured for the quantification of DB via ^{13}C NMR spectroscopy is listed in Table S1 to S7 with a comparison of observed (obsd) and estimated (estd) chemical shifts. The chemical shifts (δ) were estimated using ChemDrawUltra 12.0 software (CambridgeSoft). Estimations for chemical shifts may not be entirely accurate for every signal especially for some estimations that did not correspond exactly to a signal in the spectra. In this case, these signals were assigned in the same order as the prediction. Signals overlapping completely with a backbone signal or a main chain carbonyl signal were assigned the same chemical shift range as this main chain signal.

For *DB* quantification, the signals of interest are the C_q signal, the backbone signals and the main chain carbonyl signals. Overlapping signals of some end group signals with the polymer backbone are also accounted for as shown in Equation S1-S16. As some end group signals overlap with other signals - either backbone or other signals from the end group - some signals could not be conclusively assigned. Although a DEPT-135 spectrum was recorded, these signals were not confirmed because the corresponding carbons bear the same numbers of hydrogens.

Presence of synthesis residues like the monomer and acrylic acid (AA) dimers were also assigned. Formation of AA dimers, 2-carboxyethyl acrylate, via Michael addition reaction have been observed and investigated.[6] Signals of AA have similar chemical shift predictions to their structural counterpart in the AA dimers. No conclusive assignment can be confirmed on whether the signals observed in these predicted regions were AA or the dimers. The presence of AA dimers can be confirmed by other signals present in the molecule. Residual TFA has been observed for ATRP PAAs in this work. TFA has been used for the hydrolysis of *t*-butyl groups during the ATRP polymerization of PAA.[3]

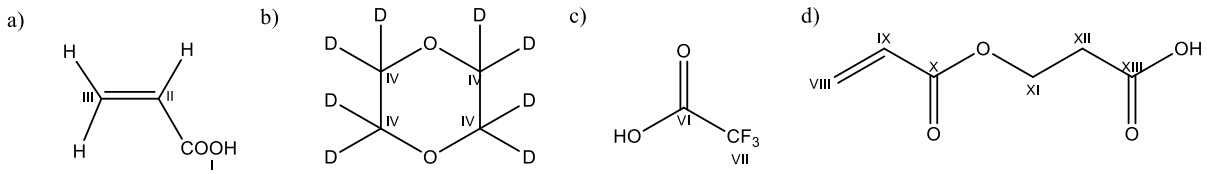

Figure S11. Chemical structure of a) AA, b) 1,4-dioxane-d_8, c) TFA and d) AA dimer labelled with the group numbers (GNs) that are used for chemical shift assignment.

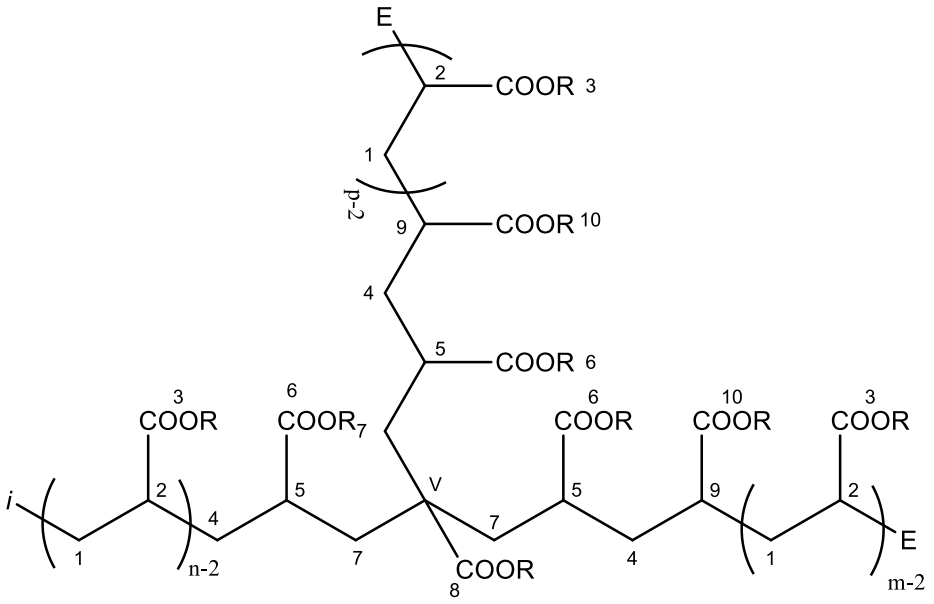

Figure S12. Chemical structure of PAAs/PNaA where R = H or R = Na. *i* represents the initiating group (see Figure S13) and E represents the chain-end (see Figure S14). The labelled GNs are used for chemical shift assignment.

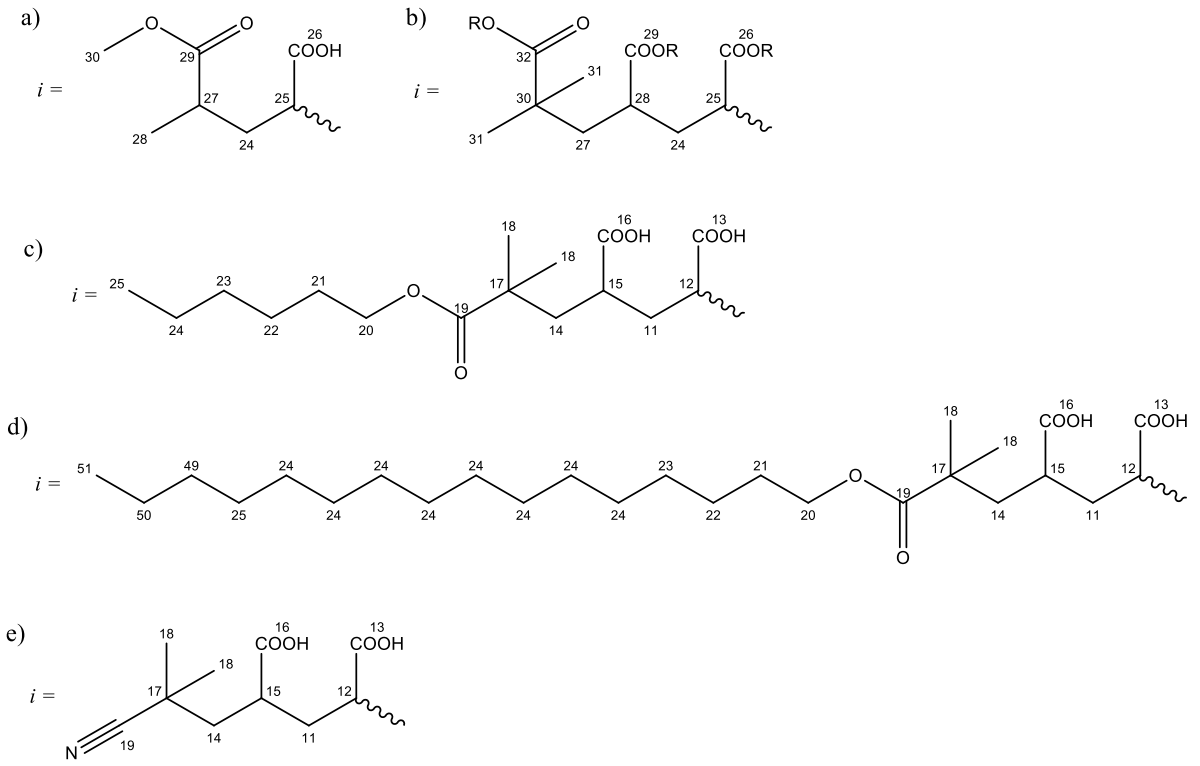

Figure S13.Chemical structure of the initiating groups (*i*) of a) MONAMS-initiated NMP PAA and MADIX PAA, b) BB-initiated NMP PAA/PNaA (where R = H or Na and will be indicated accordingly in their signal assignment table), c) hexyl 2-bromoisobutyrate-initiated ATRP PAA, d) hexadecyl-2-bromoisobutyrate-initiated ATRP PAA and e) AIBN-initiated PAA with labelled GNs that are used for chemical shift assignment.

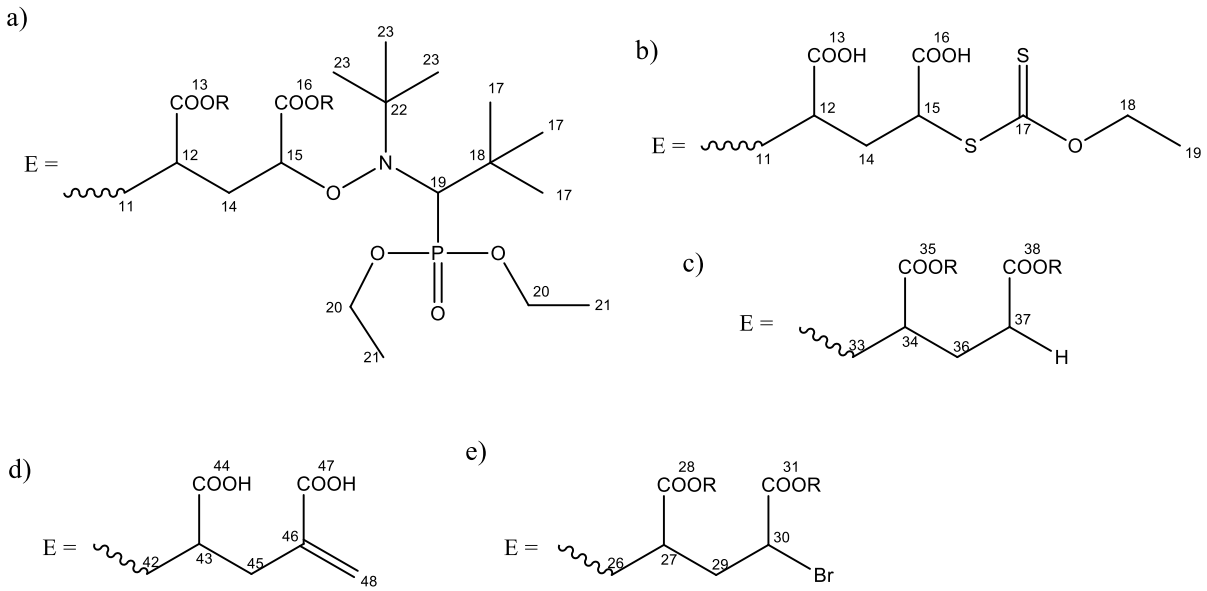

Figure S14. Chemical structure of different chain-ends (E) including the a) SG1 group, b) MADIX-agent end group, c) hydrogen, d) double-bond and e) bromine with labelled GNs that are used for chemical shift assignment.

Table S1. Signal assignment for ^{13}C NMR spectrum of NMP-AA-1 and NMP-AA-3 in 1,4-dioxane-d_8 (see Figure S2 for ^{13}C NMR spectra, see Figure S12, S13a, S14a and S14c for definition of GNs, where R=H). OL stands for overlapping, BDL for below detection limit.

GN	Estd δ (ppm)	Obsd δ (ppm), NMP-AA-1	Obsd δ (ppm), NMP-AA-3
1, 11	26.2	32.7 - 39.2	32.6 – 39.1
2, 9	41.3	39.2 - 46.8	39.1 – 44.2
3, 6, 10, 13, 26, 35	182.9	171.4 -181.9	171.9 – 180.9
4	26.5	30.0 (OL with **1**)	30.0 (OL with **1)**
5	39.1	39.9 (OL with **2**)	39.9
7	45.6	36.1 (OL with **1**)	36.0 (OL with **1**)
8	183.7	171.4 -181.9 (OL with **3**)	171.9 – 180.9 (OL with **3**)
12	37.3	39.2 - 46.8 (OL with **2**)	39.1 – 44.2 (OL with **2**)
14? 36?, XII[a]	29.4, 29.6, 33.8[b]	33.6 (OL with **1**)	33.6(OL with **1**)
15	85.8	83.5 (OL with **19**)	83.2
16	173.2	173.0 (OL with **3**)	172.9 (OL with **3**)
17	26.6	30.8 (OL with **1**)	30.7 (also OL with **1**)
18	15.3	BDL	15.4
19	81.0	83.5 (OL with **15**)	80.1
20	62.2	63.4(OL with **IV**)	63.1 (OL with **IV**)
21	16.3	16.6(OL with **28**)	16.6 (OL with **31**)
22	70.4	71.2 (OL with **IV**)	71.4 (OL with **IV**)
23	26.1	28.0 (OL with **1**)	28.3 (OL with **1**)
24? 37?[a]	27.0, 27.4	31.6 (OL with **1**)	31.6 (also OL with **1**)
25? 34?[a]	41.0, 43.5	42.7 (OL with **2**)	43.1 (OL with **2**)
27	45.6	37.9 (OL with **1**)	37.8 (OL with **1**)
28	16.9	17.5-18.4 (OL with **21**)	17.3 – 18.4 (OL with **21**)
29	176.5	175.1 (OL with **3**)	175.0 (OL with **3**)
30	52.2	51.7	51.7
33	25.9	32.7 - 39.2 (OL with **1**)	32.6 – 39.1 (OL with **1**)
38?, XIII?[a]	178.4, 177.3	177.7 (OL with **3**)	177.6
I?, X?[a]	170.4, 166.5	167.5	168.2
II?, IX?[a]	127.5, 128.2	129.6	129.6
III?, VIII?[a]	134.1, 131.3	131.3	131.2
IV	66.5	66.5	66.5
V	36.0	48.5	48.5
XI	59.8	60.7	60.7

[a]Signals corresponding to two or more estimated δ values contain OL signals. Estimated δ values are listed in the same order as respective GNs. These signals cannot be confirmed with one-dimensional NMR only and are thus indicated by a question mark. This footnote applies to every table in this section. [b]Confirmed by 2D NMR.[7]

Table S2. Signal assignment for ^{13}C NMR spectra of NMP-AA-5 and -6 in D_2O (see Figure S4 and S5 for ^{13}C NMR spectra of the polymers, respectively; see Figure S12, S13b, S14a, and S14c for definition of GNs, where R = Na). OL stands for overlapping, BDL for below detection limit.

GN	Estd δ (ppm)	Obsd δ (ppm), NMP-AA-5	Obsd δ (ppm), NMP-AA-6
1, 11	29.2	35.2 – 43.0	35.5 – 41.5
2, 9, 25	44.6	43.0 – 49.4	43.4 – 48.5
3, 6, 10, 13, 26, 29, 35	180.4	181.2 – 190.3	182.5 – 188.0
4, 24	29.5	38.9	39.5
5	42.4	46.2	47.6
7	48.6	39.7	41.2
8	179.7	181.2 – 190.3 (OL with **3**)	182.5 – 188.0 (OL with **3**)
12	40.6	44.5(OL with **2**)	45.8
14?, 36?, XII?[a]	32.4, 32.6, 33.8	35.4 (OL with **1**)	36.6 (OL with **1**)
15	88.8	84.3 (OL with **19**)	BDL
16?, 38?, VIII?, XIII?[a]	176.4, 178.0, 178.4, 177.3	181.2 – 190.3 (OL with **3**)	182.5 – 188.0 (OL with **3**)
17	26.6	28.7	28.8
18	15.3	15.3	15.3
19	81.0	84.3(OL with **15**)	BDL
20	62.2	61.9	BDL
21	16.3	16.5	16.6
22	70.4	71.5	BDL
23	26.1	27.5	26.2
27	51.5	BDL	BDL
28	41.5	43.9 – 44.9 (OL with **2**)	43.8 – 45.2 (OL with **2**)
30	41.9	43.9 – 44.9 (OL with **2**)	43.8 – 45.2 (OL with **2**)
31	24.9	25.4	25.0
32	185.1	181.2 – 190.3 (OL with **3**)	187.7(OL with 3)
33	28.9	35.2 – 43.0 (OL with **1**)	35.5 – 41.5 (OL with **1**)
34	46.8	43.0 – 49.4 (OL with **2**)	43.4 – 48.5 (OL with **2**)
37	36.3	35.2 – 43.0 (OL with **1**)	35.5 – 41.5 (OL with **1**)
I? X?[a]	170.4	176.4	176.4
II? IX?[a]	127.5	135.2[c]	135.0
III, VIII?[a]	134.1	127.1[c]	127.1
V	39.6	52.6	BDL
XI	59.8	60.0	BDL

[a]See footnote a of Table S1. [b]Confirmed by 2D NMR. [c]DEPT-135 spectrum exhibits a positive signal at 135.2 ppm corresponding to a CH or CH_3 group and a negative signal at 127.1 ppm corresponding to a CH_2 signal.

Table S3. Signal assignment for ^{13}C NMR spectra of MADIX-AA-4, -5 and -6 in 1,4-dioxane-d_8 (see Figure 1, S6 and S7 for ^{13}C NMR spectra, respectively; see Figure S12, S13a, S14b and S14c for definition of GNs, where R = H). OL stands for overlapping.

GN	Estd δ (ppm)	Obsd δ (ppm), MADIX-AA-4	Obsd δ (ppm), MADIX-AA-5	Obsd δ (ppm), MADIX-AA-6
1	26.2	32.5 – 39.5	32.3 – 39.2	32.3 – 39.3
2, 9	41.3	39.5 – 46.8	39.2 – 46.6	39.3 – 46.6
3, 6, 10, 13, 26, 35	182.9	167.8 – 183.9	167.4 – 182.3	169.9 – 182.0
4	26.5	28.9 (OL with **1**)	29.0 (OL with **1**)	29.0 (OL with **1**)
5	39.1	40.0 (OL with **2**)	39.9 (OL with **2**)	40.0 (OL with **2**)
7	45.6	36.1 (OL with **1**)	36.0 (OL with **1**)	36.0 (OL with **1**)
8	183.7	167.8 – 183.9 (OL with **3**)	167.4 – 182.3 (OL with **3**)	169.9 – 182.0 (OL with **3**)
11, 33	25.9	32.5 – 39.5 (OL with **1**)	32.3 – 39.2 (OL with **1**)	32.3 – 39.3 (OL with **1**)
12	39.9	39.5 – 46.8 (OL with **2**)	39.2 – 46.6 (OL with **2**)	39.3 – 46.6 (OL with **2**)
14? 36, XII?[a]	30.8, 29.6, 33.8	33.5 (OL with **1**)[b]	33.6 (OL with **1**)[b]	33.6 (OL with **1**)[b]
15	47.0	39.5 – 46.8 (OL with **2**)	39.2 – 46.6 (OL with **2**)	(OL with **2**) 39.3 – 46.6?
16	173.3	171.8 (OL with **3**)	171.6 (OL with **3**)	171.8 (OL with **3**)
17	215.3	212.4	212.0	212.3
18	70.0	71.1 (OL with **IV**)	70.5 (OL with **IV**)	71.2 (OL with **IV**)
19	14.0	13.7	13.7	13.7
24	27.0	29.9 (OL with **1**)	29.9 (OL with **1**)	29.9 (OL with **1**)
25	41.0	39.5 – 46.8 (OL with **2**)	39.2 – 46.6 (OL with **2**)	39.3 – 46.6 (OL with **2**)
27	35.9	37.8 (OL with **2**)	37.9 (OL with **2**)	37.9 (OL with **2**)
28	16.9	18.6	17.1	15.4
29	176.5	174.8(OL with **3**)	172.8 (OL with **3**)	172.9 (OL with **3**)
30	52.2	51.6	51.6	51.6
34	43.5	39.5 – 46.8 (OL with **2**)	39.2 – 46.6 (OL with **2**)	39.3 – 46.6 (OL with **2**)
37	27.4	31.6 (OL with **1**)	31.5 (OL with **1**)	31.6 (OL with **1**)
38?, XIII?[a]	178.4, 177.3	175.0 (OL with **3**) [b]	174.9 (OL with **3**) [b]	174.9 (OL with **3**) [b]
39[b]	[c]	57.7	-	-
40[b]	[c]	60.6	60.7	-
I?, X?[a]	170.4, 166.5	-	-	168.2 (OL with **3**)
II? IX?[a]	127.5, 128.2	-	-	129.5
III?, VIII?[a]	134.1, 131.3	-	-	131.1
IV	66.5	66.5	66.5	66.5
V	36.0	48.5	48.5	48.5
XI	59.8	-	-	60.7

[a]See footnote a of Table S1.[b]Signals XII and XIII were not present in MADIX-AA-4 and -5. OL signals only applied for MADIX-AA-6. [c]Signal not assigned due to no corresponding signals in the estimated δ values

Table S4. Signal assignment for ^{13}C NMR spectrum of ATRP-tBA-1 in 1,4-dioxane-d_8 (see Figure S8 for ^{13}C NMR spectrum, see Figure S12, S13c, S14c, and S14e for definition of GNs), where R = H). OL stands for overlapping, BDL for below detection limit. S14d is a suspected chain-end but was not confirmed as these signals either overlap or are BDL and are thus not uniquely identified.

GN	**Estd δ (ppm)**	**Obsd δ (ppm), ATRP-tBA-1**
1	26.2	32.9 – 39.2
2, 9, 12	41.3	39.2 – 46.5
3, 6, 10, 13, 16, 28, 35	182.9	173.3 – 180.4
4, 11	26.5	29.9 (OL with **1**)
5	39.1	39.2 – 46.5 (OL with **2**)
7	45.6	36.1 (OL with **1**)
8	183.7	173.3 – 180.4 (OL with **3**)
14?	50.3	39.2 – 46.5 (OL with **2**)
15?	38.5	39.2 – 46.5 (OL with **2**)
17	39.4	39.2 – 46.5 (OL with **2**)
18, 22, 26	25.2	24.2 – 27.3 (OL with **1**)
20	65.8	65.0 (OL with **IV**)
21	28.9	27.8 – 28.6 (OL with **42**)
23	31.5	29.0 (OL with **1**)
24	22.7	23.1(OL with **1**)
25	14.1	14.2
27	39.7	39.2 – 46.5 (OL with **2**)
29	33.1	32.0 (OL with **1**)
30?, 34?[a]	43.7, 43.5	39.2 – 46.5 (OL with **2**)
19?, 31?, 38?[a]	175.9[b], 178.4	173.3 – 180.4 (OL with **3**)
33	25.9	32.9 – 39.2 (OL with **1**)
36	29.6	32.9 – 39.2 (OL with **1**)
37	27.4	32.9 – 39.2 (OL with **1**)
IV	66.5	66.5
V	36.0	48.5
VI	161.4	159.2
VII	116.2	BDL

[a]See footnote a of Table S1.[b]Same estimated δ values for GNs 19 and 31.

Table S5. Signal assignment for ^{13}C NMR spectrum of ATRP-tBA-2 in 1,4-dioxane-d_8 (see Figure S9 for ^{13}C NMR spectra, see Figure S12, S13d, S14c, S14d, and S14e for definition of GNs, where R = H). OL stands for overlapping, BDL for below detection limit. S14d is a suspected chain-end but was not confirmed as these signals either overlap or are BDL and are thus not uniquely identified.

GN	**Estd δ (ppm)**	**Obsd δ (ppm), ATRP-tBA-2**
1	26.2	33.0 – 39.3
2, 9, 12	41.3	39.3 – 46.5
3, 6, 10, 13, 16, 28, 35	182.9	172.4 – 181.7
4, 11	26.5	29.4 – 31.0 (OL with **23** and **25**)
5	39.1	40.2 (OL with **2**)
7	45.6	36.1 (OL with **1**)
8	183.7	172.4 – 181.7(OL with **3**)
14?	50.3	39.3 – 46.5 (OL with **2**)
15?	38.5	39.3 – 46.5 (OL with **2**)
17	39.4	39.3 – 46.5 (OL with **2**)
18, 26	25.2	24.5 – 27.0 (OL with **22**)
19?, 31?, 38?[a]	175.9[b], 178.4	173.8 - 175.3 (OL with **3**)
20	65.8	64.9 (OL with **IV**)
21	28.9	27.6 – 29.4 (OL with **42**)
22	25.8	24.5 – 27.0 (OL with **18, 26**)
23, 25	29.3	29.4 – 31.0 (OL with **4** and **11**)
24, 36	29.6	33.0 – 39.3 (OL with **1**)
26	25.2	24.5 – 27.0 (OL with **1**)
27	39.7	39.3 – 46.5 (OL with **2**)
29	33.1	32.5 (OL with **1**)
30?, 34?[a]	43.7, 43.5	39.3 – 46.5 (OL with **2**)
33	25.9	33.0 – 39.3 (OL with **1**)
37	27.4	33.0 – 39.3 (OL with **1**)
49	31.9	31.4 (OL with **1**)
50	22.7	23.2 (OL with **1**)
51	14.1	14.3
52[c]	-[c]	80.0 – 82.6
IV	66.5	66.5
V	36.0	46.5 – 49.3
VI?	161.4	157.3 – 162.9
VII?	116.2	112.5 – 115.9

[a]See footnote a of Table S1. [b]Same estimated δ values for GNs 19 and 31. [c]Signal not assigned due to no corresponding signals in the estimated δ values.

Table S6. Signal assignment for ^{13}C NMR spectrum of CONV-AA-1 in 1,4-dioxane-d_8 (see Figure S10 for ^{13}C NMR spectrum, see Figure S12, S13e, and S14c for definition of GNs, where R = H). OL stands for overlapping.

GN	**Estd δ (ppm)**	**Obsd δ (ppm), CONV-AA-1**
1	26.2	32.6 – 39.1
2, 9, 12	41.3	39.1 – 46.8
3, 6, 10, 13, 16, 35	182.9	172.4 – 181.75
4	26.5	29.9 (OL with **1**)
5	39.1	39.9 (OL with **2**)
7	45.6	36.1 (OL with **1**)
8	183.7	172.4 – 181.75(OL with **3**)
11	26.0	32.6 – 39.1 (OL with **1**)
14	37.8	32.3 (OL with **1**)
15	38.0	37.6 (OL with **2**)
17	22.7	24.9 (OL with **1**)
18	25.4	32.6 – 39.1 (OL with **1**)
19	120.2	119.8
33	25.9	32.6 – 39.1 (OL with **1**)
34	43.5	44.8 (OL with **2**)
36?, XII?[a]	29.6, 33.8[b]	32.6 – 39.1 (OL with **1**)
37	27.4	31.6 (OL with **1**)
38?, XIII?[a]	178.4[c]	175.1(OL with **3**)
I?, X?[a]	170.4, 166.5	167.5
II?, IX?[a]	127.5, 128.2	129.6
III?, VIII?[a]	134.1, 131.2	131.2
IV	66.5	66.5
V	36.0	48.5
XI	59.8	60.6

[a]See footnote a of Table S1.

Quantitative measurement of PAA/PNaAs samples.

For this study, most PAA/PNaA for which *DB* was quantified have signals overlapping with the backbone signals, which needs to be accounted for. Equation 1 and 2 have thus been modified to equations S3 to S18. Different signals are referred to by their corresponding GNs. The slightly different chemical shifts of the signals of the backbone in the polymer were simplified to be GN1 for CH_2, GN2 for CH and GN3 for C=O for all the corresponding signals of the backbone for the equation unless specified otherwise. Note that sometimes GN 15 is not integrated together with the other backbone signals as its chemical shift is too different. Table S7 indicates which equations were used to quantify *DB* in each sample.

$$DB\ (\%) = \frac{I(\mathrm{C_{q,GNV}})\times 2\times 100}{I(C_{\mathrm{q,GNV}})+I(\mathrm{C_{q,GNV}+CH_{2,GN1}+CH_{GN2}-CH_{GN15}+CH_{3,GN17,GN23}+CH_{2,GNXII}})-5I(\mathrm{CH_{3,GN30}})-I(\mathrm{CH_{2,GNXI}})} \quad \text{(S3)}$$

$$DB\ (\%) = \frac{I(\mathrm{C_{q,GNV}})\times 100}{I(\mathrm{C{=}O_{GN3}+C{=}O_{GN29}+C{=}O_{GNXIII}})-I(\mathrm{CH_{3,GN30}})-I(\mathrm{CH_{2,GNXI}})} \quad \text{(S4)}$$

$$DB\ (\%) = \frac{I(\mathrm{C_{q,GNV}})\times 2\times 100}{I(\mathrm{C_{q,GNV}})+I(\mathrm{C_{q,GNV}+CH_{2,GN1}+CH_{GN2}-CH_{GN15}+C_{GN30}+CH_{2,GNXII}})-I(\mathrm{CH_{2,GNXI}})} \quad \text{(S5)}$$

$$DB\ (\%) = \frac{I(\mathrm{C_{q,GNV}})\times 100}{I(\mathrm{C{=}O_{GN3}+C{=}O_{GN32}+C{=}O_{GNVIII}+C{=}O_{GNXIII}})-I(\mathrm{C_{GN18}})-2I(\mathrm{CH_{2,GNXI}})} \quad \text{(S6)}$$

$$DB\ (\%) = \frac{I(\mathrm{C_{q,GNV}})\times 2\times 100}{I(\mathrm{C_{q,GNV}})+I(\mathrm{C_{q,GNV}+CH_{2,GN1}+CH_{GN2}+C_{GN27}})-I(\mathrm{CH_{3,GN28}})} \quad \text{(S7)}$$

$$DB\ (\%) = \frac{I(\mathrm{C_{q,GNV}})\times 100}{I(\mathrm{C{=}O_{GN3}+C{=}O_{GN29}})-I(\mathrm{CH_{3,GN28}})} \quad \text{(S8)}$$

$$DB\ (\%) = \frac{I(\mathrm{C_{q,GNV}})\times 2\times 100}{I(\mathrm{C_{q,GNV}})+I(\mathrm{C_{q,GNV}+CH_{2,GN1}+CH_{GN2}+C_{GN27}})-I(\mathrm{CH_{3,GN19}})} \quad \text{(S9)}$$

$$DB\ (\%) = \frac{I(\mathrm{C_{q,GNV}})\times 100}{I(\mathrm{C{=}O_{GN3}+C{=}O_{GN29}})-I(\mathrm{CH_{3,GN19}})} \quad \text{(S10)}$$

$$DB\ (\%) = \frac{I(\mathrm{C_{q,GNV}})\times 2\times 100}{I(\mathrm{C_{q,GNV}})+I(\mathrm{C_{q,GNV}+CH_{2,GN1}+CH_{GN2}+C_{GN27}+CH_{2,GNXII}})-I(\mathrm{CH_{3,GN19}})-I(\mathrm{CH_{2,GNXI}})} \quad \text{(S11)}$$

$$DB\ (\%) = \frac{I(\mathrm{C_{q,GNV}})\times 100}{I(\mathrm{C{=}O_{GN3}}+\mathrm{C{=}O_{GN29}}+\mathrm{CH_{2,GNXIII}})-I(\mathrm{CH_{3,GN19}})-I(\mathrm{CH_{2,GNXI}})} \quad \text{(S12)}$$

$$DB(\%) = \frac{I(\mathrm{C_{q,GNV}})\times 2\times 100}{I(\mathrm{C_{q,GNV}})+I(\mathrm{C_{q,GNV}}+\mathrm{CH_{2,GN1}}+\mathrm{CH_{GN2}}+\mathrm{CH_{2,GN17,GN21-24}}+\mathrm{CH_{3,GN18}})-7I(\mathrm{CH_{3,GN25}})} \quad \text{(S13)}$$

$$DB\ (\%) = \frac{I(\mathrm{C_{q,GNV}})\times 100}{I(\mathrm{C{=}O_{GN3}}+\mathrm{C{=}O_{GN19}})-I(\mathrm{CH_{3,GN25}})} \quad \text{(S14)}$$

$$DB(\%) = \frac{I(\mathrm{C_{q,GNV}})\times 2\times 100}{I(\mathrm{C_{q,GNV}})+I(\mathrm{C_{q,GNV}}+\mathrm{CH_{2,GN1}}+\mathrm{CH_{GN2}}+\mathrm{CH_{2,GN17-18,GN21-25,GN49-50}})-17I(\mathrm{CH_{3,GN51}})} \quad \text{(S15)}$$

$$DB\ (\%) = \frac{I(\mathrm{C_{q,GNV}})\times 100}{I(\mathrm{C{=}O_{GN3}}+\mathrm{C{=}O_{GN19}})-I(\mathrm{CH_{3,GN51}})} \quad \text{(S16)}$$

$$DB\ (\%) = \frac{I(\mathrm{C_{q,GNV}})\times 2\times 100}{I(\mathrm{C_{q,GNV}})+I(\mathrm{C_{q,GNV}}+\mathrm{CH_{2,GN1}}+\mathrm{CH_{GN2}}+\mathrm{C_{GN17}}+\mathrm{CH_{3,GN18}}+\mathrm{CH_{2,GNXII}})-3(CN_{\mathrm{GN19}})-I(\mathrm{CH_{2,GNXI}})} \quad \text{(S17)}$$

$$DB\ (\%) = \frac{I(\mathrm{C_{q,GNV}})\times 100}{I(\mathrm{C{=}O_{GN3}}+\mathrm{C{=}O_{GNXIII}})-I(\mathrm{CH_{2,GNXI}})} \quad \text{(S18)}$$

Table S7. Equations used for *DB* quantification of PAAs and PNaAs

Sample	Equations
NMP-AA-1 and -3	S3[a], S4
NMP-AA-5	S5[a],S6[a]
MADIX-AA-4	S7[b], S8[b]
MADIX-AA-5	S9[a, b], S10[a, b]
MADIX-AA-6	S11[a], S12[a]
ATRP-tBA-1	S13, S14
ATRP-tBA-2	S15, S16
Conv-AA-1	S17, S18

[a]Calculation was based on the assumption of 100 % livingness. [b]Equations S7 and S9, as well as Equations S6 and S8 can be used interchangeably for their respective samples; however, the assigned equation was preferred due to stronger signals present for that specific equation.

Peak area-to-noise ratio (*PNR*) and its precision

The normalized *PNR* of toluene was determined to assess the precision of this method to estimate the extent of dissolution. The samples were known to contain toluene at the same concentration, as toluene was used as an internal standard to assess starch dissolution.[8] Toluene is known to be fully miscible in the solvent used, DMSO. The *PNR* values were normalized with respect to the concentration ([toluene]) used and to the square root of the number of scans (*NS*):

$$PNR_{\text{norm}} = \frac{PNR \times \sqrt{NS}}{[\text{toluene}]} \qquad \text{(S19)}$$

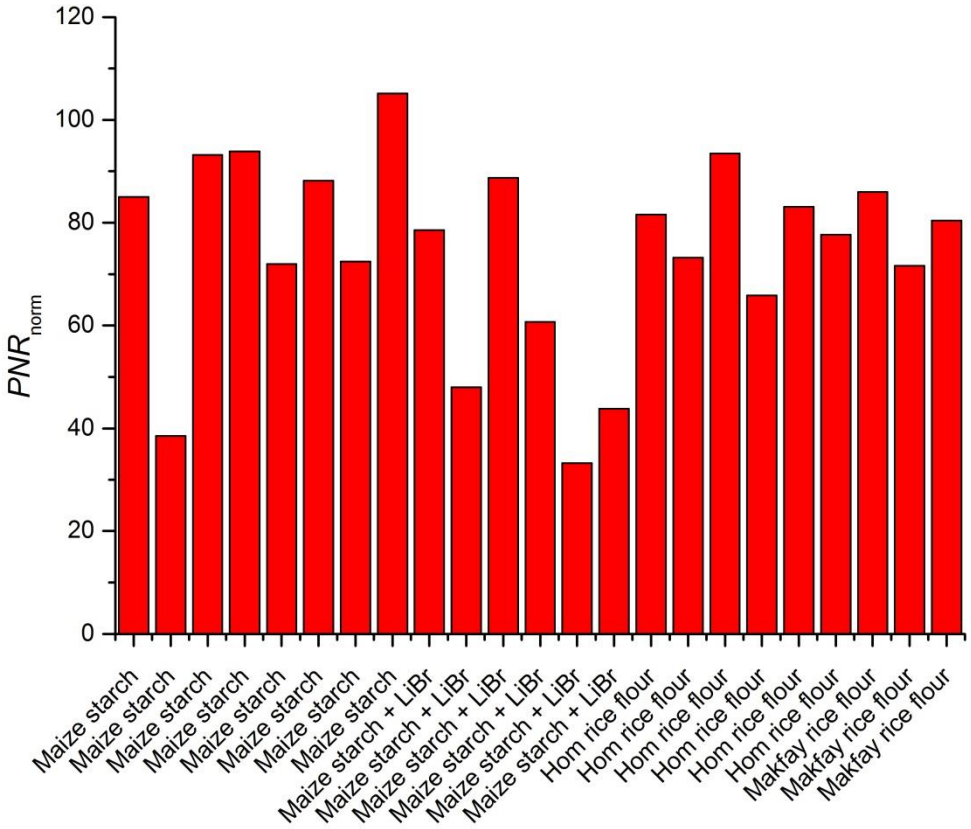

Figure S15. Comparison of the normalized *PNR* values obtained for toluene present as an internal standard in different starch solutions.[8] The graph labels are starch sample names. Each sample was prepared once and measured at least 4 times (as shown by adjacent bars on the graph).

^{1}H NMR for dissolution studies

Quantitative ^{1}H NMR spectra of PAAs/PNaAs were measured to investigate the dissolution of some PAAs/PNaAs (Table S9). Several representative, quantitative ^{1}H NMR spectra are shown in Figure S16 to S18.

Table S8. Dissolution conditions of PAAs/PNaAs samples for ^{1}H NMR spectroscopy, as well as moisture content *mc*, mass fraction of end groups and acrylic acid, f_{eg} and f_{AA} respectively used in the determination of the extent of their dissolution. To investigate the effect of viscosity on the solubility of these samples, these samples were also diluted by a factor of 10.

Sample	Solvent	C_{nom} (g·L^{-1})	*mc* (%)	f_{eg}	f_{AA}
NMP-AA-3	1,4-dioxane-d_8	150	6.87	0.00252	<LOD
NMP-AA-5	D_2O	149	13.08	0.00361	0.294
NMP-AA-6	D_2O	100	22.13	0.00181	0.312
NMP-AA-6[a]	D_2O / NaOD[b]	74.9	22.13	0.00181	0.279
NMP-tBA-1	D_2O	125	5.09	0.00245	0.00685
NMP-tBA-1	DMSO-d_6	69.9	5.09	0.00245	0.00629
MADIX-AA-5[a]	1,4-dioxane-d_8	200	6.32	0.04687	<LOD
Linear	D_2O	100	20.44	0.000	<LOD

[a]Dissolved at 60 °C and 300 rpm for 1 h.

[b]NaOD is 1 mol equivalent to acrylic acid units

[c]<LOD = Below the limit of detection

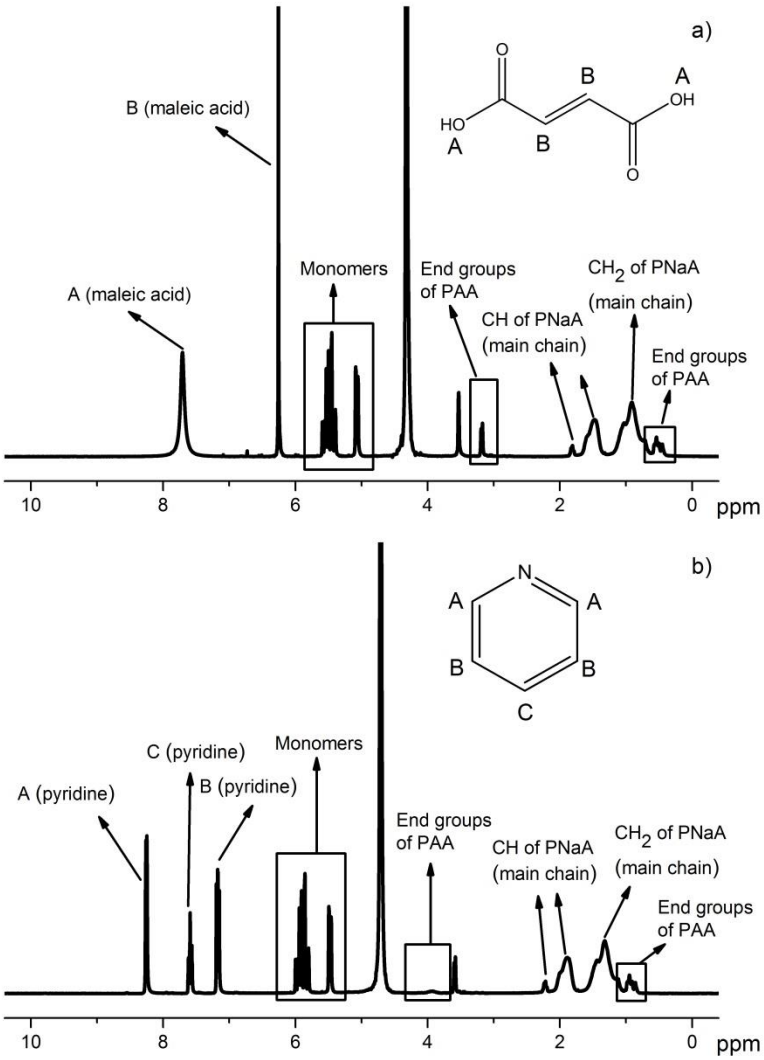

Figure S16. ^{1}H NMR spectra of NMP-AA-6 with a) maleic acid and b) pyridine as internal standard. The chemical structure of each internal standard is shown on the corresponding spectrum. Signals at ≈ 3.5 and 4.3 ppm correspond to solvent signal of 1,4-dioxane-d_8 and D_2O respectively.

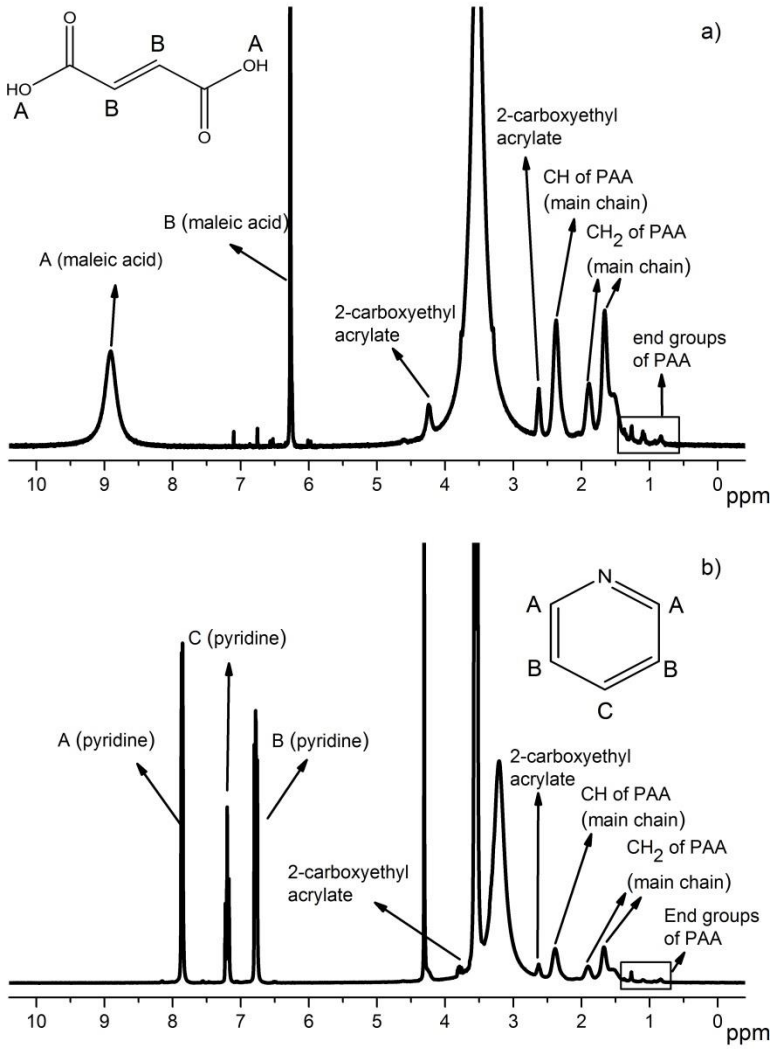

Figure S17. ^{1}H NMR spectra of MADIX-AA-5 with a) maleic acid and b) pyridine as internal standard. Signals at ≈ 3.5 and 4.3 ppm correspond to solvent signal of 1,4-dioxane-d_8 and D_2O respectively. The 2-carboxy ethyl acrylate labels identify signals of the 2-carboxy ethyl acrylate monomer unit incorporated in the polymer.

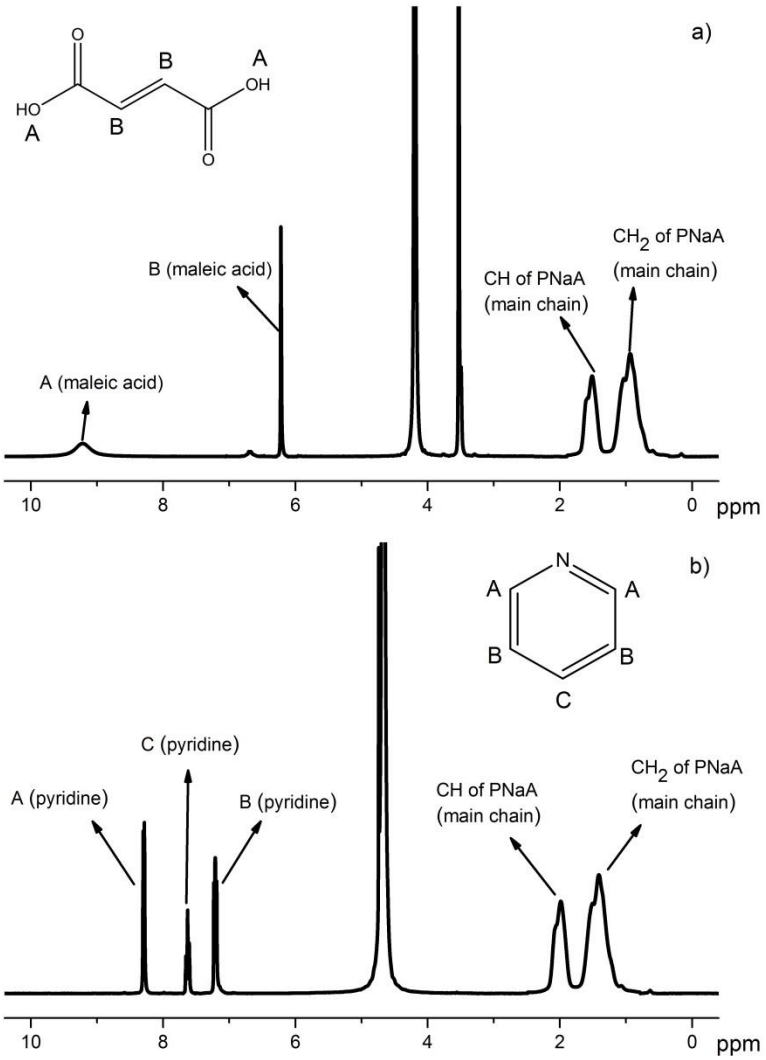

Figure S18. ^{1}H NMR spectra of Linear with a) maleic acid and b) pyridine as internal standard. Signals at ≈ 3.5 and 4.3 ppm correspond to solvent signal of 1,4-dioxane-d_8 and D_2O respectively.

Assessment of the precision of $\%_{diss}$ due to data treatment

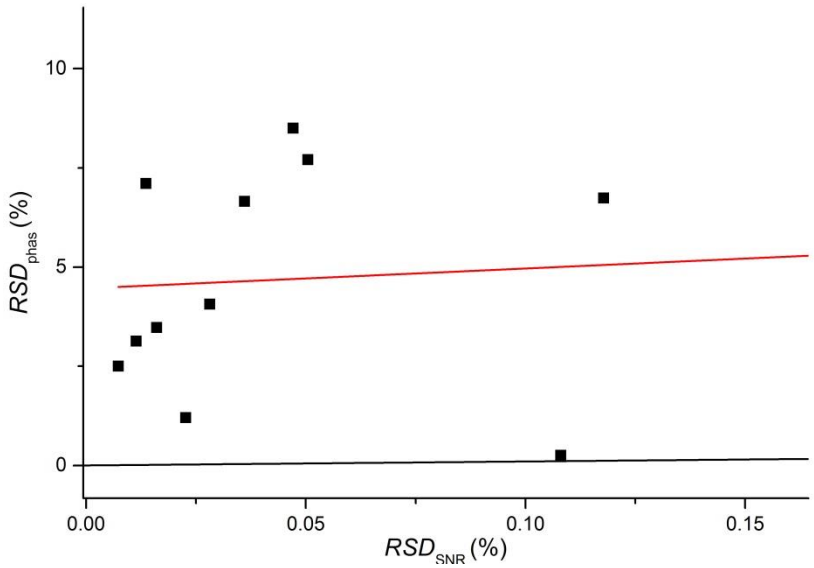

Figure S19. Comparison of errors originating in the limited *SNR* and in the data treatment (phasing) for the $\%_{diss}$ of PAAs/PNaAs (^{1}H NMR experiments). The linear fit is shown in red ($y = 5.01x + 4.46$, $R^2 = 0.0171$), the diagonal in black.

Dissolution of PAAs/PNaAs

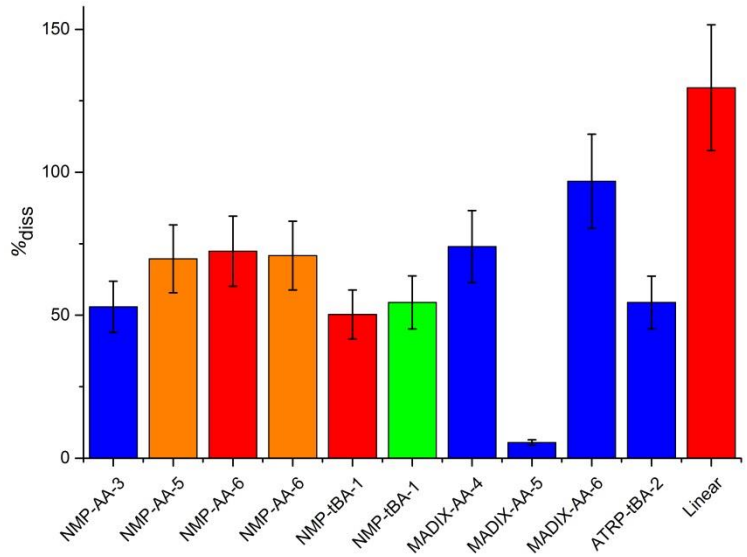

Figure S20. Dissolution of several PAAs and PNaAs in different solvents including 1,4-dioxane-d_8 (blue), D_2O with NaOD (orange), D_2O (red) and DMSO-d_6 (green) using maleic acid as an internal standard. Some $\%_{dissolved}$ values are overestimated due to sample evaporation.

TGA of PAAs/PNaAs

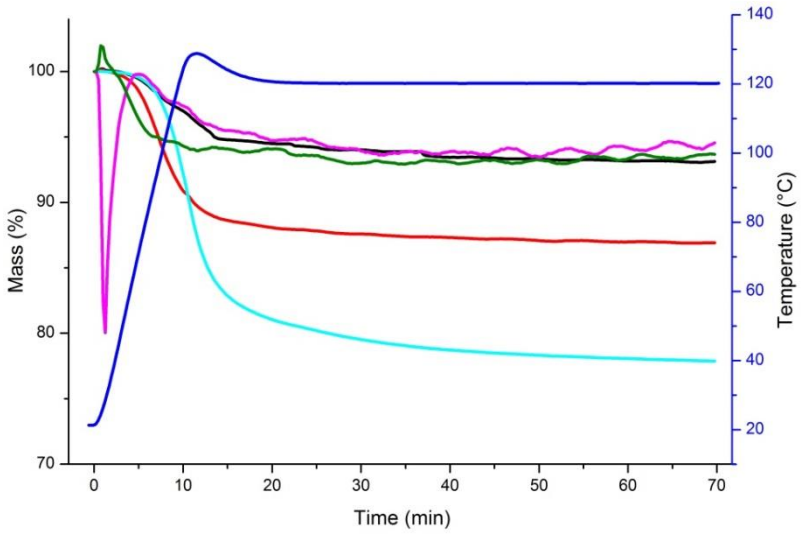

Figure S21. TGA thermogram of NMP-AA-3 (black), NMP-AA-5 (red), NMP-AA-6 (cyan), NMP-tBA-1 (pink), MADIX-AA-5 (olive) and the temperature (blue) over time.

REFERENCES:

1. Maniego, A. R.; Ang, D.; Guillaneuf, Y.; Lefay, C.; Gigmes, D.; Aldrich-Wright, J. R.; Gaborieau, M.; Castignolles, P. Separation of poly(acrylic acid) salts according to the topology using capillary electrophoresis in the critical conditions, *Analytical and Bioanalytical Chemistry* **2013,** 405, 9009-9020.
2. Sutton, A. T.; Read, E.; Maniego, A. R.; Thevarajah, J. J.; Marty, J.-D.; Destarac, M.; Gaborieau, M.; Castignolles, P. Purity of double hydrophilic block copolymers revealed by capillary electrophoresis in the critical conditions, *Journal of Chromatography A* **2014,** 1372, 187-195.
3. Wallace, A. D.; Al-Hamzah, A.; East, C. P.; Doherty, W. O. S.; Fellows, C. M. Effect of Poly(acrylic acid) End-Group Functionality on Inhibition of Calcium Oxalate Crystal Growth, *Journal of Applied Polymer Science* **2010,** 116, 1165-1171.
4. East, C. P.; Wallace, A. D.; Al-Hamzah, A.; Doherty, W. O. S.; Fellows, C. M. Effect of Poly(acrylic acid) Molecular Mass and End-Group Functionality on Calcium Oxalate Crystal Morphology and Growth, *Journal of Applied Polymer Science* **2010,** 115, 2127-2135.
5. Claridge, T. D. W., Chapter 2 Introducing high-resolution NMR. In *High-Resolution NMR Techniques in Organic Chemistry*, Elsevier: Oxford, England, 2009; Vol. 27, pp 11-34.
6. Fujita, M.; Iizuka, Y.; Miyake, A. Thermal and kinetic analyses on Michael addition reaction of acrylic acid, *Journal of Thermal Analysis and Calorimetry* **2016**, 1-7.
7. Sutton, A. T.; Arrua, R. D.; Gaborieau, M.; Castignolles, P.; Hilder, E. F. Characterization of oligo(acrylic acid)s and their block co-oligomers, *in preparation* **2017**.
8. Schmitz, S.; Dona, A. C.; Castignolles, P.; Gilbert, R. G.; Gaborieau, M. Assessment of the Extent of Starch Dissolution in Dimethyl Sulfoxide by 1H NMR Spectroscopy, *Macromolecular Bioscience* **2009,** 9, 506-514.